Electrochemical oxidation treatment of Direct Red 23 aqueous solutions: Influence of the operating conditions

Fatima Ezzahra Titchou, Hicham Zazou, Hanane Afanga, Jamila El Gaayda, Rachid Ait Akbour, Geoffroy Lesage, M. Rivallin, Marc Cretin, Mohamed Hamdani

Electrochemical oxidation treatment of Direct Red 23 aqueous solutions: Influence of the operating conditions

Fatima Ezzahra Titchou[a,*], Hicham Zazou[a], Hanane Afanga[a], Jamila El Gaayda[a], Rachid Ait Akbour[a], Geoffroy Lesage[b], Matthieu Rivallin[b], Marc Cretin[b,*], Mohamed Hamdani[a,*]

[a] Ibn Zohr University, Faculty of Sciences, Chemical department, BO 8106 –Dakhla district, Agadir, Morocco.

[b] Institut Européen des Membranes, IEM, Univ Montpellier, CNRS, ENSCM, Montpellier, France

*Corresponding authors:

marc.cretin@umontpellier.fr (M. Cretin)

hamdani.mohamed@gmail.com (M. HAMDANI)

titchoufatimaezzahra@gmail.com (F.E. TITCHOU)

Abstract

A comparative study of the degradation of Direct Red 23 (DR23) dye aqueous solutions by electrooxidation was investigated using different anodes: carbon graphite (CG), dimensionally stable anode (DSA), Magnéli phase Ti_4O_7, and boron doped diamond (BDD). Stainless steel (SS) and CG plates were tested as cathodes. The effect of operating parameters on the degradation kinetic of the dye was studied. In this study, NaCl and Na_2SO_4 were selected as supporting electrolytes; the former was found to be more suitable for the degradation of DR23. The degradation of the dye follows a pseudo-first-order kinetic in both media. Higher total organic carbon (TOC) efficiency was achieved by BDD/CG cells. Thus, the treatment efficiency obtained using a current density of 5 mA cm^{-2}, and DR23 concentration of 60 mg L^{-1} was about 86 % using both NaCl and Na_2SO_4 electrolyte, at 6 h electrolysis time. The energy consumptions per g TOC removed were found to be 2.05 and 2.6 kWh g^{-1} TOC in NaCl and Na_2SO_4 electrolytes, respectively.

Keywords: Electrooxidation, Direct Red 23 dye, organic degradation, mineralization, wastewater treatment.

1. Introduction

Nowadays, organic dye pollutants become a serious threat to the environment. Even in a small quantity, they present a source of turbidity, eutrophication, non-aesthetic pollution; and their discharge is particularly troublesome. Dyes present a higher biochemical stability due to their high molecular weight and aromatic rings which are difficult to eliminate [1]. Azo dyes constitute a real problem to the aqueous system and human health due to their side effects such as carcinogenicity, skin irritation, allergy, acute toxicity, and mutagenicity [2,3]. Several means were investigated to treat wastewaters containing recalcitrant pollutants; conventional ones are usually ineffective. Although usual treatments such as precipitation,

biodegradation coupled to membrane separation, coagulation, flocculation, adsorption [4–7], and electrocoagulation [8–12] were experienced for discoloration, they have common drawbacks of generating sludge [8,13]. To overcome these problems, electrochemical advanced oxidation processes (EAOPs) present a promising way to treat persistent pollutants [2,14,15] due to the unique characteristics such as high efficiency, high mineralization, and nonhazardous waste produced [3]. The interest related to EAOPs application for water treatment is linked to their easy manipulation being ecofriendly methods. In terms of sustainability, their installations can be supplied by renewable energies [16–18]. These technologies are easily automatable, viable, decentralizable and finally adaptable according to the nature of the effluents to be treated. The duration of the treatment can be optimized according to the biorefractoriness of the effluent to finally end up with a biodegradable solution after treatment [19]. The driving force is the in-situ generation of highly oxidant agents mainly $^{\bullet}OH$ radicals with a higher oxidation potential (versus standard hydrogen electrode (SHE)) $E°$ ($^{\bullet}OH/H_2O$) = 2.80 V/ SHE [20–22]. These reactive entities are able to destroy unselectively organic and organometallic contaminants until their complete mineralization into CO_2, water, and inorganic ions [23,24]. They are considered the main oxidizing species for the removal of organic pollutants in EAOPs, where hydroxyl radicals can be generated in the bulk solution (homogeneous $^{\bullet}OH$, denoted $^{\bullet}OH$) and/or at the anode surface (heterogeneous $^{\bullet}OH$, marked $M(^{\bullet}OH)$, where M refers to anode material) [25,26]. Depending on the used anode and its potential window for water discharge, $M(^{\bullet}OH)$ may be physisorbed in case of non-active anodes and chemisorbed in case of active anodes [24–26].

Electrochemical oxidation (electrooxidation) is an environmentally friendly method for the treatment of water and wastewater, constitutes a direct way to produce $M(^{\bullet}OH)$ radicals without using chemicals, where electrons are the only reagents [27]. $^{\bullet}OH$ production generally requires higher O_2 overpotential anodes (M) (Eq. (1)) [2]. Several electrodes have been used

for the electrooxidation such as PbO_2, doped SnO_2, IrO_2, DSA (dimensionally stable anodes) that are mainly mixed metal oxide anodes, or Pt and BDD (boron doped diamond) [20]. SnO_2 and PbO_2 electrodes have a short life-time service and release toxic ions to the solution [1]. Pt electrode is expensive which prevents it from being used for the scale-up. On the other hand, BDD, a non-active anode, presents a wide potential window for water discharge; that provides a promising condition for industrial-scale wastewater treatment. This anode is able to generate weakly physisorbed hydroxyl radical [1]. Moreover, it can generate relatively weak oxidants such as reactive oxygen species O_3 and H_2O_2, chlorine species, peroxodisulfate ($S_2O_8^{2-}$), peroxodiphosphate ($P_2O_8^{4-}$), or peroxodicarbonate ($C_2O_6^{2-}$) species [28–31]. This non-active anode exhibits a good chemical and electrochemical stability and a long life time service [1]. DSA, an active anode, formed by a mixture of metal oxides, has the property of generating hydroxyl radicals and a higher electrocatalytic activity for chlorine evolution reaction [32]. This property is due to the redox reaction of the transition metal elements which act as active sites for chlorine atom adsorption [1]. Comparing BDD and DSA activity, unlike BDD, DSA has low ability to electro-generate M(•OH). It has a high stability, large production of Cl_2, and chlorine-oxygen species, which are endowed with lower oxidant power than •OH, but with interesting activity [33]. Therefore, direct oxidation of organics presents a sluggish kinetic reaction on DSA surface and the secondary reaction is favored [1]. Recently, ceramic electrodes based on sub-stoichiometric TiO_2, especially, Ti_4O_7 were reported to be an alternative to BDD anodes. They are characterized by a high electrical conductivity and a low-cost due to their preparation using TiO_2, the most abundant feedstock on the planet [34]. Moreover, concerning their electrochemical efficiency, they behave as non-active anodes, yielding to a higher electrochemical mineralization efficiency compared to DSA [35,34]. Table 1 shows a brief summary of the recent application of electrooxidation in the treatment of targeted organic pollutants.

$$M(H_2O) \rightarrow M(^{\bullet}OH) + H^+ + e^- \qquad (1)$$

(Table 1)

Considering the negative effect of dyes to the environment, this paper aimed to study the degradation and mineralization of Direct Red 23 (DR23) as an azo naphthalene dye from its aqueous solution. It is well known that azo dyes, containing a double bond N=N, are toxic and their by-products are carcinogenic and mutagenic to the life being. According to this, previous papers reported its elimination using photocatalytic degradation [41–45], UV-assisted AOPs [46], persulfate oxidation [47], UV/H_2O_2 process using carbon nanotube particles [48,49], adsorption process [50], enzymatic process [51], photo-electro Fenton [52,53], electro Fenton [54], ozonation and ultrasonolysis processes [55]. Nevertheless, the degradation and mineralization of DR23 using electrooxidation remain unstudied. Electrooxidation, the most popular and low cost technique, is considered as an effective technique to treat dyeing solutions since it can degrade it by in-situ M($^{\bullet}$OH) generation and/or by mediating active oxidants [56]. It does not need any chemical reagent addition such as Fe^{2+} unlike the electro-Fenton process. Electrooxidation efficiency depends on the operating conditions such as temperature, pH, electrolyte medium, and electrode materials [33,56–58]. Therefore, this work aims to study the discoloration and mineralization of DR23 aqueous solution using electrooxidation as the most widely used and powerful electrochemical process. To the best of our knowledge, degradation/incineration of this dye is not yet performed. This study compared the efficiency of its removal using different powerful known anodes. BDD anode is known by its higher potential for the removal of organic pollutants. However, it main drawback is its higher cost. Therefore, this comparative study can be useful to highlight the possible use of other powerful anodes in order to achieve similar efficiencies of those of BDD anode. The effect of different operating conditions was studied under galvanostatic mode using different anode/cathode cells in chloride and sulfate media. As the concentration of salts

(electrolytes) differs form an industry to another, the chosen concentrations fall in the range of the used amounts in textile industry, presenting the minimum of supporting electrolyte that promotes the easy follow of discoloration kinetic and prevents side reactions and ohmic drop [59,60]. The amount of salts 25 mM NaCl (conductivity = 2.5 mS cm^{-1}) and 12.5 mM Na_2SO_4 (conductivity = 2.3 mS cm^{-1}) were chosen to perform all the experiments in a constant 25 g-equivalent of supporting electrolyte medium. Discoloration experiments of the dye solutions were achieved in various operating conditions using different anode materials to compare their efficiency for the removal of DR23. The range of tested parameters was chosen based on some pretests and on different relevant literatures [23,61]. Mineralization efficiency, based on total organic carbon (TOC) measurement, mineralization current efficiency (MCE%), and energy consumption during the electrolysis were investigated.

2. Materials and methods

Direct Red 23 (DR23), the chosen pollutant to formulate the synthetic wastewater, is generally used in viscose cellulose fiber dyeing for silk, wool, paper, and pulp dyeing. It is an azo naphthalene dye ($C_{35}H_{25}N_7Na_2O_{10}S_2$, molar mass of 813.73 g mol^{-1}, color index C.I. 29160), of analytical grade, purchased from Sigma Aldrich and used without any further purification. Required amount of DR23 was dissolved in ultrapure water to prepare the desired concentrations. Sodium hydroxide, sulfuric acid, sodium chloride, and sodium sulfate, were analytical grades from Prolabo and Fluka. All solutions were prepared with ultrapure water obtained from a Millipore Milli-Q system with resistivity > 18 MΩ cm at 25 °C.

2.1. Description of the electrochemical process

The elimination of DR23 by electrooxidation, in a batch study, was carried out with 230 mL of the dye solution in a 250 mL Pyrex beaker. The electrolysis was performed in an undivided

electrolytic cell where different electrode combinations were used. All used electrodes except for Ti_4O_7 anode were purchased from different suppliers. Four anodes were tested: dimensionally stable anode (DSA), (Ti/RuO_2–IrO_2 (4 cm × 6 cm × 0.2 cm) from Baoji Xinyu Guang Ji Dian Limited Liability Company, China), which can be prepared as reported by Yu et al. [62], boron doped diamond (BDD) thin-film deposited on a niobium substrate (4 cm × 6 cm × 0.2 cm) from CONDIAS, Germany, fabricated as described by Fryda et al. [63], carbon graphite (CG)(expanded graphite sheet PSB-860, (4 cm × 6 cm × 0.4 cm), purchased from SHIELD SEALING & Packing CO., LTD, China, prepared as indicated by Liu et al. [64], and Ti_4O_7 (4 cm × 6 cm × 0.2 cm) thin film deposited on Ti substrate from Saint Gobain Research Provence (France) prepared as described elsewhere [65,66]. Ti_4O_7 was synthesized by plasma coating of prepared TiO_x (x < 2) particles (20–60 μm) on a Ti substrate (4 cm × 6 cm) as described by Ganiyu et al. [65]. Ti substrate surface was pretreated by sandblasting in order to obtain a rough surface. By applying coating conditions reported by Ganiyu et al. [65], a continuous thick film of 100 μm and 95% density was achieved. The prepared electrode mainly contains Ti_4O_7 phase with the presence of TiO_2 rutile and Ti_3O_5 as indicated by X-ray diffraction. The plasma-sprayed coating has a typical electronic conductivity of 10^3 S cm^{-1}. The tested cathodes were CG (4 cm × 6 cm× 0.4 cm), and AINSI 304 Stainless steel (SS) plate (4 cm × 6 cm × 0.4 cm). Electrolysis was conducted under galvanostatic conditions, by applying a constant current using a digital DC supply unit, ELC model ALR3002M. For all electrodes, 30 cm^2 is kept constant as the submerged geometric surface area. The distance between these electrodes was 1.5 cm, and they were connected to the DC power supply. The pH variation was monitored using HANNA pH meter. Prior to each experiment, compressed air (Flow air, 1.5 L min^{-1}) was bubbled for 10 min through the cell to saturate the solution with dissolved oxygen. All electrolyses were performed in triplicate and averaged at room

temperature (20 ±2 °C), and the solutions were homogenized with magnetic stirring (600 rpm) during the treatment to allow efficient mass transfer.

2.2. **Analytical procedure**

The discoloration was monitored using Shimadzu spectrophotometer UV-VIS 1800 at the maximum adsorption wavelength (λ_{max} = 502 nm), to assess the decrease in chromophore absorption bands by taking different aliquots of 2 mL at different times. Calibration curve of DR23 absorbance was prepared using known aqueous solutions with different concentrations (20, 30, 40, 60, 80, 100, and 200 mg L^{-1}). The color removal was computed using (Eq. (2)):

$$\text{Color removal (\%)} = \left(\frac{A_0 - A_t}{A_0}\right) \times 100 \qquad (2)$$

where A_0 and A_t are the initial and final dye absorbance.

Total Organic Carbon (TOC) measurements were determined by injecting samples of 50 µL through thermal catalytic oxidation at 680 °C using TOC-L SHIMADZU analyzer equipped with a manual injector. The TOC removal was then calculated using (Eq. (3)):

$$\text{TOC removal (\%)} = \frac{TOC_0 - TOC}{TOC_0} \times 100 \qquad (3)$$

where TOC_0 and TOC stand for the initial and TOC (mg L^{-1}) at a given reaction time, respectively.

The mineralization current efficiency, MCE%, was estimated by (Eq. (4)) [67]:

$$MCE\% = \frac{nFVs\Delta(TOC)_{exp}}{4.32\times10^{7}\times m\times I\times t} \times 100 \qquad (4)$$

where F is the Faraday constant (96487 C mol^{-1}), V_S is the solution volume (L), $\Delta\ (TOC)_{exp}$ is the experimental TOC change (mg L^{-1}) at a given time, 4.32×10^7 is an homogenization factor

(3600 s h^{-1}× 12,000 mg of C mol^{-1}), m is the number of carbon atoms of DR23 (35 atoms), I is the applied current (A) and t is the electrolysis time (h). n is the electron transfer number per mole of DR23 taken as 138 considering the total mineralization according to the following reaction Eq. (5):

$$C_{35}H_{25}N_7Na_2O_{10}S_2 + 68\ H_2O \rightarrow 35\ CO_2 + 133\ H^+ + 2\ Na^+ + 7\ NH_4^+ + 2\ SO_4^{2-} + 138\ e^- \quad (5)$$

The energy consumption, EC, (kWh g^{-1} TOC) was determined using (Eq. (6)) [68]:

$$EC\ (kWh\ g^{-1}\ TOC) = \frac{E_{cell}\ It}{(TOC_0 - TOC_t)V_s} \quad (6)$$

where E_{cell} is the average voltage applied (V), I is the applied current intensity (A), t is the treatment time (h), TOC_0 and TOC_t are the TOC values (mg L^{-1}) at the initial time and at a given electrolysis time t, respectively, and V_s is the solution volume (L). In all trials, degradation was monitored using UV-Vis technique while mineralization was followed by TOC-meter.

3. Results and discussion

3.1. Parameters influencing the degradation of DR23

3.1.1. Effect of electrode materials and supporting electrolyte

Although electrooxidation is a process essentially based on the power of the anode in the electrolytic cell, the cathode can help improve the efficiency of the process, which depends on the nature of the electrode used. The electrode materials influence the degradation rate of organic pollutants since their efficiency depends on their ability to generate oxidizing species such as M(•OH) and/or chlorine and sulfate active species on the anode and H_2O_2 on the cathode. The former species are the main oxidizing agents for the destruction of pollutants. Therefore, this study focused on the role of the nature of the anode and cathode materials in addition to the supporting electrolyte to set the effective combination to get rid of DR23.

Therefore, four anodes including dimensionally stable anode (DSA), boron-doped diamond (BDD), Ti_4O_7, and CG, were tested and compared using CG, and stainless steel (SS) as cathodes. The degradation was carried out using 40 mg L^{-1} DR23, 8.3 mA cm^{-2} current density, and 25 mM NaCl or 12.5 mM Na_2SO_4, at natural pH (pH = 6.0), to set the effect of electrode combination, Figure 1. In all cases, color removal increased progressively with electrolysis time and this increase depends on the added salt. In these trials, the pH remained almost constant with variations close to ± 0.3 pH units in Na_2SO_4 medium, whereas it changes in NaCl where the final pH evolves to be near to neutral at the end of electrolysis, in the case of BDD and DSA, and acidic for Ti_4O_7. The drop of the pH to acidic values using Magnéli Ti_4O_7 may have a beneficial effect on the stability of hydroxyl radicals that requires acidic conditions [69]. Similar observation was already reported by Salazar et al. [33] indicating that the active chlorine evolution changes the final pH of the solution as a function of electrodes and electrolysis time.

Comparing the activity of anode materials, DSA, Ti_4O_7, and BDD anodes show a higher degradation activity compared to CG, whatever the medium. Although the CG anode may contribute to the degradation of DR23 by the M($^{\bullet}$OH) radicals formed, during electrolysis, its surface burns over time, damaging it and limiting its reuse. Carbon-based materials such as CG undergo incineration, and their corrosion depends on various parameters such as pH, current and the presence of NaCl. This corrosion occurs even at low currents [70,71].

Regarding the electrolytic media, the higher discoloration activity was found in NaCl supporting electrolyte. In the presence of sulfate ions, compared to DSA anode, BDD and Ti_4O_7 are known being able to generate reactive sulfate species, $S_2O_8^{2-}$ and $SO_4^{\bullet-}$, depending on the pH and applied current density, through direct oxidation on the anode surface or the reaction with M($^{\bullet}$OH) (Eqs. (7)-(15)(12)) [72–76]. The electro-generated sulfate active species may contribute to the solution degradation in addition to the strong oxidant M($^{\bullet}$OH)

radicals [72,77–79]. However, for DSA, the lower degradation efficiency could be attributed to the strong adsorption of M(•OH) that can limit the discoloration rate [33].

$$2SO_4^{2-} \rightarrow S_2O_8^{2-} + 2e^- \quad (7)$$

$$HSO_4^- \rightarrow S_2O_8^{2-} + 2H^+ + 2e- \quad (8)$$

$$2SO_4^{\bullet-} \rightarrow S_2O_8^{2-} \quad (9)$$

$$SO_4^{\bullet-} + SO_4^{2-} \rightarrow S_2O_8^{2-} + e^- \quad (10)$$

$$SO_4^{2-} \rightarrow SO_4^{\bullet-} + e^- \quad (11)$$

$$S_2O_8^{2-} + e^- \rightarrow SO_4^{\bullet-} + SO_4^{2-} \quad (12)$$

$$2SO_4^{2-} + 2\,M(^{\bullet}OH) + 2H^+ \rightarrow M + S_2O_8^{2-} + 2H_2O \quad (13)$$

$$SO_4^{2-} + M(^{\bullet}OH) \rightarrow M + SO_4^{\bullet-} + OH^- \quad (14)$$

$$HSO_4^- + M(^{\bullet}OH) \rightarrow SO_4^{\bullet-} + H_2O \quad (15)$$

These sulfate active species are known by their higher standard potential being 2.01 V/SHE for $S_2O_8^{2-}$ and 2.6 V/SHE for $SO_4^{\bullet-}$ [72,80,81]. However, the higher bleaching properties of chloride active species compared to sulfate active species are reported in many cases. For example, the effects of different electrolytes (NaCl, Na_2SO_4, Na_2CO_3, and $HClO_4$) on Alizarin Red S (ARS) degradation using BDD anode, were studied and compared. A fast complete discoloration of ARS was achieved within 6 min using NaCl electrolyte [82].

Regarding the obtained results, the NaCl supporting electrolyte was used for further investigations on the degradation of DR23.

In the case of BDD and DSA anodes, the presence of NaCl leads to generate electro-active chlorine oxidizing species such as Cl_2, HClO, and ClO^-, once chloride ions undergo oxidation

as reported by Degaki et al. [83] and Jalife-Jacobo et al. [56] following the reactions (Eqs. (16)-(19)). Furthermore, the low evolution of chlorine on DSA surface favors the generation of active chlorine species during the oxidation of chlorides [68].

$$2Cl^-(aq) \rightarrow Cl_2(aq) + 2\ e^- \quad (16)$$

$$Cl^-(aq) + {}^{\bullet}OH \rightarrow HOCl(aq) + e^- \quad (17)$$

$$Cl_2 + H_2O \leftrightarrow HOCl(aq) + Cl^-(aq) + H^+(aq) \quad (18)$$

$$HOCl(aq) \leftrightarrow ClO^-(aq) + H^+(aq) \quad (19)$$

It should be noted that the stability of these oxidizing agents in the solution depends on its pH. The pk_a of $HOCl/ClO^-$ couple is given equal to 7.55 [68]. Globally, chlorine, Cl_2 is the predominant species when pH < 3.00, hypochlorous acid, HOCl for 3.00 < pH < 7.50, and hypochlorite ion, ClO^- for pH > 7.55 [67,84]. However, other species of chlorine, ClO_2^-, ClO_3^- and ClO_4^-, with low oxidizing power were mentioned in the literature [85].

However, in the case of Ti_4O_7, the oxidation of Cl^- according to Eq. (16) do not occurs on Ti_4O_7 surface as reported by Wang et al. [86]. They reported that the degradation of organics is mainly attributed to $M({}^{\bullet}OH)$ radicals formed at the anode surface beside the synergic effect of chlorine active species formed as follow: (Eqs. (20)-(24)).

$$M({}^{\bullet}OH) + Cl^- \leftrightarrow ClHO^{\bullet-} + M \qquad k = 4.3 \times 10^9\ M^{-1}\ s^{-1} \quad (20)$$

$$ClHO^{\bullet-} + H^+ \rightarrow Cl^{\bullet} + H_2O \qquad k = 2.1 \times 10^{10}\ M^{-1}\ s^{-1} \quad (21)$$

$$Cl^{\bullet} + Cl^- \leftrightarrow Cl_2^{\bullet-} \qquad k = 6.5 \times 10^9\ M^{-1}\ s^{-1} \quad (22)$$

$$Cl^{\bullet} + Cl^{\bullet} \rightarrow Cl_2 \qquad k = 8.8 \times 10^7\ M^{-1}\ s^{-1} \quad (23)$$

$$Cl_2 + H_2O \rightarrow Cl^- + HOCl + H^+ \qquad k = 15\ M^{-1}\ s^{-1} \quad (24)$$

Moreover, in terms of reactivity, they reported that hydroxyl radicals are more reactive than the produced chlorine species. Their lower reactivity leads to their accumulation in the cell

with less oxidation potential to form ClO^-, ClO_2^-, ClO_3^-, and ClO_4^- as presented in Eqs. ((25)-(28)) [87].

$$Cl^{\bullet} + M(^{\bullet}OH) \rightarrow ClO^- + e^- + H^+ \quad (25)$$

$$ClO^- + M(^{\bullet}OH) \rightarrow ClO_2^- + e^- + H^+ \quad (26)$$

$$ClO_2^- + M(^{\bullet}OH) \rightarrow ClO_3^- + e^- + H^+ \quad (27)$$

$$ClO_3^- + M(^{\bullet}OH) \rightarrow ClO_4^- + e^- + H^+ \quad (28)$$

Regarding the negative impact of ClO_3^- and ClO_4^- on health (disturbation of the normal functions of the thyroid gland and carcinogenic effect) [86], the low production of these species in the case of Ti_4O_7 present an advantage for this electrode for their large scale application in electrooxidation of organic pollutants [86].

As it can be seen in Figure 1**,** the highest degradation of DR23 is obtained using DSA/CG system in the presence of chloride ions. In this case, the discoloration of the solution results mainly from the dye's chromophore destruction by active chlorine species which are formed at the testing pH solution. Similar results are carried out by others studying the degradation of Reactive Blue 19 dye using a BDD or DSA anode in a flow reactor [83].

The oxidation power of DSA/CG and DSA/SS are almost similar, the difference is due to the contribution of CG cathode which may generate H_2O_2 (Eq. (29)) unlike the SS cathode which promotes mainly oxygen reduction via 4 transferred electrons. It is well known that cathodes made of carbon materials promote the formation of H_2O_2 via two-electron oxygen reduction reaction (ORR) at low current density according to the reaction (Eq. (29)) [88,89]. The generation of oxidant species, H_2O_2 on the cathode is more favorable in acidic medium. In addition, carbonaceous materials have significant catalytic performance for accelerating the activation of in-situ generated H_2O_2 into hydroxyl radicals that enhances the degradation and mineralization efficiency [90,91].

$$O_2 + 2\ H^+ + 2\ e^- \leftrightarrow H_2O_2 \qquad E^O = 0.695\ V\ /SHE \qquad (29)$$

Sopaj et al. [92] stated that the stainless steel cathode generates very low H_2O_2 amounts, for the operating conditions, current densities of 2.4 to 5 mA cm^{-2}, Pt anode, 50 mM Na_2SO_4, pH = 3.00, under continuous air bubbling conditions. In the previous work, the hydrogen peroxide amount was determined by titration of the complex (1:1) formed between Ti(IV) and H_2O_2 by measuring its color intensity in acidic media, at a wavelength of 423 nm.

Likewise, the difference of discoloration efficiency obtained for both Ti_4O_7 and BDD using CG and SS cathodes could be interpreted by the generation of H_2O_2 on CG surface. As presented in the Figure 1, the discoloration in the case of Ti_4O_7 is almost coincident with that of DSA. Similar result was observed by He et al. [93] using Ti_4O_7 and DSA anode for the discoloration of methyl orange solution. In NaCl medium, the discoloration follows the order: DSA/CG ≈ Ti_4O_7/CG > DSA/SS ≈ Ti_4O_7/SS > BDD/CG > BDD/SS. The lower degradation in the case of Ti_4O_7 and BDD compared to DSA anode can be attributed to the consumption of M(•OH) due to chlorine (Eqs. ((25)-(28)) [34]. In contrast, active anodes, endowed with high oxygen evolution overpotential, the oxidation of target molecules mainly occurs directly on the anode surface by the adsorbed hydroxyl radicals electro-generated according to reaction (Eq. (1)). However, the oxidation rate strongly depends on the applied current density and mass transfer in the cell as the pollutants must reach the anode surface [1]. It was reported that the oxidation of pollutants by M(•OH) generated by inactive anodes leads to high removal efficiency; these reacting species are adsorbed physically onto the anode surface and react with the pollutant in the interface of solid/solution [94,95]. Hence, the treatment cost may increase according to the electrolysis time. The use of effective intermediate oxidizing agents obtained by electro-generating active chlorine species leads to indirect oxidation by mass transfer to the bulk of the solution, which hinders the above limitation. Based on these assertions, color removal is principally dependent on the active chlorine species

concentrations produced by the used electrodes as suggested by Salazar et al. [33]. These authors recognized that the production of chlorine species on DSA anodes is higher than what was generated on BDD anodes whatever the pH and current density. Similar results were carried out by Malpass et al. [96] using BDD and DSA anodes for the degradation of both the pesticide atrazine and cyanuric acid by electrooxidation in NaCl and Na_2SO_4 supporting electrolytes. Therefore, DSA, Ti_4O_7, or BDD anode, and CG as the cathode were chosen to study the operating conditions effect on the degradation of DR23 for the sake of comparison in NaCl medium.

(Figure 1)

3.1.2. Effect of NaCl concentration

The study of NaCl electrolyte deserves special attention since Cl^- has an ubiquitous character [15]. The electrical conductivity of the solution plays an important role in the degradation reaction. Good conductivity leads to a faster electron transfer, a better degradation ratio, and energy saving [8,69]. In chloride media, the reduction of organic compounds occurs mainly by indirect oxidation other than direct oxidation, due to strong in-situ electro-generated reactants, which may transform target pollutants into less harmful compounds. As was already reported before, the main oxidizing agents are active chlorine, hypochlorous acid, or hypochlorite ions, those reactants are produced anodically from chloride as indicated in reactions (Eqs. ((16)-(19)) [1,8]. It is well known that increasing the concentration of the supporting electrolyte affects color removal, which positively impacts the conductivity of the solution and reduces the cell voltage leading to decrease the energy consumption.

To study the effect of supporting electrolyte on the removal of 60 mg L^{-1} of DR23, different concentrations of NaCl, 12.5, 25, 50, and 75 mM were investigated. Experiments were carried

out under 5 mA cm^{-2} current density and at natural pH of the solution (pH = 6.0 ± 0.4), for DSA/CG, Ti_4O_7/CG, and BDD/CG cells, as shown in Figure 2a, 2b, and 2c, respectively**.** The same behavior was observed for DSA, Ti_4O_7, and BDD, the color removal increases when the concentration of NaCl increases, illustrating the positive impact on the degradation of DR23. The enhancement of the efficiency is related to the increase of production-mediated oxidants and the decrease of the selectivity for oxygen evolution due to the increase of Cl^- concentration as reported by Jager et al. [39].

The total discoloration requires 40 min for a concentration of 12.5 mM of NaCl where it requires only 20 min using 50 mM or 75 mM of NaCl in all electrolytic cells tested. On the other hand, the discoloration rate is slower for BDD/CG system compared to DSA/CG and Ti_4O_7/CG, in the same operating conditions. The kinetic of discoloration fits with the pseudo-first order kinetic model with R^2 almost equal to unity. As shown in Figure 2d, the kinetic rates enhance from 0.080 to 0.173 min^{-1}, from 0.079 to 0.197 min^{-1}, and from 0.069 to 0.1514 min^{-1} when the concentration of NaCl increases from 12.5 to 75 mM, for Ti_4O_7, DSA and BDD, respectively. The higher kinetic rate in the case of DSA anode and especially for 75 mM of NaCl is related to the higher accumulation of active chlorine species formed in the medium. This behavior is in complete agreement with the reported literature of the degradation of organic compounds being enhanced with NaCl concentration [97–100]. As mentioned by Ganiyu et al. [73] the generation of reactive chlorine species is particularly high using DSA anodes. However, in the case of BDD, less active chlorine species can be simultaneously generated by the action of M($^{\bullet}$OH) according to the reactions (Eqs. ((25)-(28)), where ClO_3^- and ClO_4^- are considered as unwanted by-products [85,101]. These species were endowed with low oxidizing power, they limit the electrochemical degradation of organics and constitute a scavenger for hydroxyl radicals as reported by Dominguez et al. [85]. Furthermore, the higher kinetic rates in the case of Ti_4O_7 may be attributed to the less

formation of ClO_3^- and ClO_4^- and the stability of hydroxyl radicals under acidic conditions as mentioned before.

(Figure 2)

3.1.3. Effect of current density

The current density is a direct controlled parameter; it affects the degradation rate and the energy consumption. Figure 3a, 3b, and 3c present the current density variation effect on the elimination rate of 60 mg $L^{-1}$of DR23 using 25 mM of NaCl at pH = 6.0 for DSA, BDD, and Ti_4O_7 anodes, respectively. The increase in the current density enhances the color removal and regulates the ability of hydroxyl radical and active chlorine generation on anode surfaces [56,102,103]. The total discoloration occurred around 40 min for a density of 2.5 mA cm^{-2} and decreased to be only 10 min using 15 mA cm^{-2} on the tested anodes. However, the discoloration is almost faster in the case of DSA/CG system; this is due to the greater electro-generation of active chlorine species [1]. The apparent kinetic rates increased about three times from 0.055 to 0.291 min^{-1}, from 0.045 to 0.237 min^{-1}, and from 0.0831 to 0.182 min^{-1} when the current density increased from 2.5 to 15 mA cm^{-2}, for DSA/CG, BDD/CG, and Ti_4O_7/CG cells, respectively, Figure 3d. Similarly, the electrochemical oxidation kinetic rate of Acid Brown 98 using Ti/$Ru_{0.3}Ti_{0.7}O_2$ composite anode increases from 0.036 to 0.062 min^{-1} when the current density increases from 5 to 20 mA cm^{-2} [99]. Likewise, Paniza et al. [1] investigated a comparison between indirect oxidation on DSA anode and direct oxidation on BDD surface of Acid Brown 98, they reported that the degradation enhanced with increasing the current density for both electrodes while the discoloration of the solution is almost faster on DSA anode. Regarding K_{app} values, Ti_4O_7 anode leads to a faster degradation compared to DSA and BDD anode in similar operating conditions under lower current densities (2.5 and 5 mA cm^{-2}). However, applying a current density above 5 mA cm^{-2} could not further increase

the discoloration of DR23 solutions in the case of Ti_4O_7, where the apparent kinetic rates exhibit little changes. For higher current densities (10 and 15 mA cm^{-2}) K_{app} follows the order: K_{app} (DSA) > K_{app} (BDD) > K_{app} (Ti_4O_7). This result was consistent with the degradation of tetracycline using Ti/Ti_4O_7 anode [104]. This behavior can be attributed to the limited mass transfer rate of DR23 toward the Ti_4O_7 at a higher current density and/or, to some extent, enhances some side reactions such as O_2 evolution and increases the energy consumption [104,105].

(Figure 3)

3.1.4. Effect of the concentration of DR23

Figure 4a, 4b, and 4c present the effect of the concentration of DR23 on the color removal, using 25 mM NaCl and 5 mA cm^{-2} as the current density. As the concentration of dyes in textile wastewater is ranged from 5 to 230 mg L^{-1} as reported by Yaseen et al. [60], the tested concentrations of DR23 were 60, 80, 100, and 200 mg L^{-1}. The increase of the initial concentration decreases either the efficiency of the discoloration, Figure 4a, 4b, and 4c, and the kinetic rate Figure 4d. The apparent kinetic rate constants decreased from 0.101 to 0.070 min^{-1}, from 0.093 to 0.065 min^{-1}, and from 0.134 to 0.046 min^{-1} when the concentrations of DR23 increased from 60 to 200 mg L^{-1} in DSA/CG, BDD/CG, and Ti_4O_7/CG cells, respectively. Generally, longer times of treatment are required to attain the same color removal efficiency with the increase of the initial concentration of DR23, due to the considerable slower discoloration rate at higher pollutant load [2]. This behavior can be related to the greater amount of organics in solution to react with the similar amount of oxidizing species, associated with the propensity of dye molecules to form clusters at high concentration, thus decreasing dye diffusion rate to the anode surface [106]. With the increase of DR23 concentration, the accumulation of intermediates and by-products is expectable,

which are thereafter competing with the colored compounds to react with the same amount of active chlorine in the case of DSA and either with M(•OH) in the case of BDD and Ti_4O_7 anodes. Consequently, a smaller proportion of organics compared to the initial pollutant concentration is oxidized. Abdel-Aziz et al. [106] reported that increasing the initial concentration of dyes from 50 to 100 mg L^{-1} decreased the color removal from 60 to 41% and from 70 to 46% for methylene blue and methyl blue, respectively, during the first 10 min of treatment using 2.5 g L^{-1} of NaCl at pH = 3 and under 42.55 mA cm^{-2}. Similar behavior was also reported elsewhere with increasing concentration of organic pollutants [98].

(Figure 4)

3.1.5. Effect of initial pH

Figure 5a, 5b, and 5c present the effect of initial pH on the color removal of 60 mg L^{-1} of DR23 using 25 mM NaCl under a current density of 5 mA cm^{-2}. The higher color removal efficiency is achieved at pH = 3.00 using DSA/CG system. When the initial pH increased, the effectiveness of the degradation decreases dramatically by increasing the pH from 5.00 to 11.00. For BDD/CG cell, the effectiveness of the degradation remains sensibly constant in the pH range of 3.00 to 9.00, while it decreased slightly at pH = 11.00. Therefore, the direct oxidation of DR23 on the BDD anode is efficient over a wide pH range. Serrano [107] reported the effect of acidic pH on the performance of the discoloration of the solution and explained the faster oxidation in the presence of active chlorine. This behavior is related to oxidizing power given by the standard potential of each produced chloride species, i.e. HOCl and Cl_2 have the highest standard potential (E° ($HOCl/Cl^-$) = 1.49 V/SHE) compared to Cl_2 (E° (Cl_2/Cl^-) = 1.36 V/SHE) and ClO^- (E° (ClO^-/Cl^-) = 0.89 V/SHE). In addition, Rajkumar et al. [98] attributed the decrease of the efficiency of the elimination of Reactive Blue 19 in chloride medium using DSA anode to the decreased production of chlorine/hypochlorite at

higher pH conditions, due to the formation of chlorate or perchlorate with a low oxidizing potential according to the following reactions (Eqs. (30), (31)).

$$6\ HOCl + 3\ H_2O \rightarrow 2\ ClO_3^- + 4\ Cl^- + 12\ H^+ + 3/2\ O_2 + 6\ e^- \quad (30)$$

$$ClO_3^- + H_2O \rightarrow ClO_4^- + 2\ H^+ + 2\ e^- \quad (31)$$

The pH variation during electrolysis can be attributed to the formation of these species (insert panels (Figure 5a and 5b)). In the case of the Magnéli phase Ti_4O_7 (Figure 5c), the degradation of DR23 was highly influenced by the initial pH value. The best efficiency was obtained for pH = 3 and it decreased with increasing the pH value. After 30 min of electrolysis time the discoloration achieved was 97%, 97%, 95%, 94%, and 84% using pH 3, 5, 7, 9, and 11, respectively.

The pH drops during the first 30 min in the case of Ti_4O_7 contrarily to the case of using DSA and BDD anodes (insert panel (Figure 5c)). This behavior can be attributed to the slow formation of ClO_3^- and ClO_4^- on the surface of Ti_4O_7 due to the absence of direct oxidation of Cl^-, where it is mainly oxidized according to Eq. (20) and (21) [86]. This fact was also observed by Wang et al. in the case of perfluoroalkyl acids treatment using Ti_4O_7, where they reported that no appreciable chlorate and perchlorate was formed during the first 8 h of the treatment [87]. Similar results was observed by Gui et al. [108] in the case of methyl orange degradation.

Wang et al. [86] observed the higher accumulation of free chlorine using Ti_4O_7 compared to BDD anode suggesting their less readily oxidation potential on the Ti_4O_7, which highlights its advantage in application for electrochemical oxidation treatment of organic pollutants in chloride medium.

However, to ensure the maximum mineralization efficiency in the subsequent part, the solution pH will be adjusted to acidic (pH = 3.00) during the electrolysis. In general, it is well known that hydroxyl radical formation is better in acidic media [26,69]. Therefore, the higher efficiency at various solution pH promotes the practical implementation of electrooxidation process to treat wastewaters.

(Figure 5)

3.2.Mineralization

3.2.1. Effect of electrode system on the mineralization efficiency of DR23

To determine the best treatment to eliminate DR23 by electrooxidation, the mineralization efficiency was investigated. Figure 6 presents a comparison of the mineralization efficiency of DR23 in terms of TOC removal, using different electrode systems. Operating conditions were fixed at 60 mg L^{-1} of DR23, pH = 3.00, 5 mA cm^{-2} with 25 mM of NaCl (Figure 6a) or 12.5 mM of Na_2SO_4 (Figure 6b). The pH value was maintained at 3.0 ± 0.3 by adding acidic solution during the electrolysis time, in the case of NaCl medium. As shown in Figure 6a and 6b, TOC removal increased steadily for about 1.5 h before slowing down with prolonged electrolysis time. The highest rate of TOC removal was achieved using BDD/CG system, around 86% using either NaCl or Na_2SO_4 electrolytes, after 6 h of electrolysis. Meanwhile, BDD/SS system, whose activity comes just below the former, presents the mineralization efficiency of 73 and 82 % in NaCl and Na_2SO_4 electrolytes, respectively, under similar experimental conditions. It is evidenced that the use of CG cathode enhanced the breakdown of DR23 in NaCl medium, with a relative increase of 18%, unlike Na_2SO_4, which may be attributed to the activity of CG cathode to generate H_2O_2, contributing to the mineralization of the dye. Furthermore, for all other systems, the use of CG cathodes allows higher TOC

449 removals than those of SS cathodes, in the same operating conditions. DSA/CG cell, endowed
450 with a good activity in degradation, presents the worst mineralization efficiencies in chlorine
451 and sulfate medium; they reached only 25 and 28 % TOC removal respectively. Between the
452 two extreme results, Ti_4O_7/CG, Ti_4O_7/SS, CG/SS and CG/CG systems present intermediate
453 efficiencies. However, Ti_4O_7/CG and Ti_4O_7/SS yield to a close efficiency to that of BDD
454 anode in NaCl medium. After 6h of electrolysis time, TOC removals achieved using
455 Ti_4O_7/CG and Ti_4O_7/SS were 60 and 51% in NaCl and 44 and 42% in Na_2SO_4, respectively.
456 CG/SS and CG/CG reached 36 and 39 % in NaCl electrolyte and reached 45 and 51 % in
457 Na_2SO_4 electrolyte, respectively. Several authors have suggested that the mineralization
458 process is improved using a chloride ion as a supporting electrolyte [20,56]. Oturan [25]
459 reported that BDD thin film anode has a higher oxidation and/or mineralization power for the
460 treatment of organic pollutants in sulfate medium. This is due to the generation of physisorbed
461 M(•OH) which are more available for destruction of organics than in the case of metallic
462 oxide anodes and DSA. Active anodes such as DSA and graphite have a low value of oxygen
463 evolution overpotential and permit only the partial oxidation of organics [109]. Salazar et al.
464 [33] compared the mineralization of Disperse Yellow 3 dye on BDD, Ti/$Ru_{0.3}Ti_{0.7}O_2$, and
465 Ti/Pt anodes in Na_2SO_4 and NaCl supporting electrolytes and achieved 90% TOC removal
466 with BDD in sulfate solution, while the percentage is up to 50% for other anodes, irrespective
467 of the operating conditions. They reported that DSA anode is more active in NaCl medium,
468 followed by BDD and Ti/Pt due to higher production of effective chlorine species which
469 depend on pH and anode material. Likewise, Yang et al. [110] reported that the order of the
470 mineralization of Imatinib drug decreases in the order: BDD > Ti_4O_7 > Pt > DSA. They
471 evaluated the TOC removal efficiency in Na_2SO_4 media, achieving total mineralization at 8 h
472 treatment using BDD anode. They also mentioned that the mineralization rate was 61%, 78%,
473 and 82% by Pt, DSA, and Ti_4O_7 anodes, respectively.

DR23 mineralization in BDD/CG system is mainly occurred by direct and mediated electrochemical oxidation on the BDD surface in sulfate and in chloride media, respectively. Physisorbed M(•OH) radicals, the strong oxidant, are considered as the main oxidant in sulfate solution, while homogenous oxidation prevails in the chloride solution in the bulk of the solution or near the anode surface. The trend of the TOC removal curve obtained by BDD/CG in NaCl medium, Figure 6a, unlike in Na_2SO_4, Figure 6b, shows that the mineralization can still increase with the electrolysis time, confirming that the by-products are still breakdown. Jalife-Jacobo et al. [56] have found the same results studying the degradation of diazo dye congo red on BDD/SS cell and reported a favorable synergy between the free M(•OH) and the active chlorine species leading to a faster mineralization using NaCl. On the other hand, various by-products may be formed which are highly recalcitrant to oxidation by the action of M(•OH) generated conjugated to that of oxidant species such as persulfates in Na_2SO_4 medium.

Based on (Eq. (6)), the energy consumption per g of TOC removed is presented in Figure 6c using different electrode cells at 5 mA cm^{-2} after 6h electrolysis time. The energy consumption, EC, at the end of electrolysis using BDD/CG is lower compared to other systems. It is about 2.05 and 2.60 kWh g^{-1} TOC for NaCl and Na_2SO_4, respectively. The same trends which corroborate our findings were already reported [33]. This result highlights clearly the low EC and the efficiency of BDD anode for DR23 treatment in solutions containing chloride salts.

(Figure 6)

3.2.2. Effect of current on the mineralization efficiency

The effect of current density on TOC removal in the case of BDD/CG is presented in Figure 7a and 7b for NaCl and Na_2SO_4, respectively. In the case of NaCl (Figure 7a), increasing the current density from 2.5 to 15 mA cm^{-2} increases the TOC removal value and reduce the time required for total mineralization. After 6h, the obtained TOC removal values were 80%, 86%, 94%, and 95% using 2.5, 5, 10, and 15 mA cm^{-2}, respectively. On the other hand, in the case of Na_2SO_4, the variation of TOC removal (%) vs. current density is shown in Figure 7b. As can be seen from the results, the increase of current density over 5 mA cm^{-2} does not significantly improve the TOC removal % after 6h of electrolysis. The mineralization reached was74%, 86%, 91%, and 92% using 2.5, 5, 10, and 15 mA cm^{-2}, respectively. The uncompleted mineralization can be attributed to the formation of recalcitrant and toxic by-products like chloroderivatives that are slowly degraded by active chlorine species and M($^{\bullet}$OH), in the case of NaCl. In addition, the TOC removal efficiency can be affected by the consumption of M($^{\bullet}$OH) by sulfate (Eqs.(13)-(15)) or chloride ions (Eq. (20)), and the decomposition of H_2O_2 by HOCl or $SO_4^{\bullet-}$ (formed through the reaction between sulfate ions and $^{\bullet}$OH (Eqs. (14), (15)) as presented in Eqs. (32)-(34) [111].

$$HClO + H_2O_2 \rightarrow Cl^- + O_2\,(g) + H_2O + H^+ \quad (32)$$

$$SO_4^{\bullet-} + H_2O_2 \rightarrow SO_4^{2-} + H^+ + HO_2^{\bullet} \quad (33)$$

$$SO_4^{\bullet-} + HO_2^{\bullet} \rightarrow SO_4^{2-} + H^+ + O_2 \quad (34)$$

Besides the increase of the kinetic of TOC removal with the current density, the mineralization current efficiency, MCE%, deceased by increasing applied current density values, Figure 7c and 7d. MCE% values were significant for 2.5 mA cm^{-2} at 2h of electrolysis; they were about 7.5% and 5.2% for NaCl and Na_2SO_4, respectively. For both electrolytes, increasing the electrolysis time reduces the MCE% due to the formation of short chain carboxylic acids that resist to the mineralization [61]. The increase in the current density

enhances the side reaction of oxygen evolution on BDD surface (Eq. (35)) as well as the recombination of $^{\bullet}OH$ in the bulk (Eq. (36)) or oxidation of M($^{\bullet}OH$) at the anode (Eq. (37)) [21].

$$H_2O \rightarrow 1/2\ O_2 + 2\ H^+ + 2\ e^- \quad (35)$$

$$2\ ^{\bullet}OH \rightarrow H_2O_2 \quad (36)$$

$$2\ M\ (^{\bullet}OH) \rightarrow O_2 + 2\ H^+ + 2\ e^- \quad (37)$$

To evaluate the feasibility of the process and the reliability of the electrodes, the energy consumption, EC (kWh g^{-1} TOC) was computed using (Eq. 4) and its trend is presented in Figure 7e and 7f. The increase of current density increases the energy consumption with electrolysis time. It is clear from Figure 7e and 7f that 5 mA cm^{-2} requires a low EC, about 2.05 kWh g^{-1} TOC and 2.6 kWh g^{-1} TOC using NaCl and Na_2SO_4, respectively, to achieve 86 % of TOC removal after 6h of electrolysis. From MCE% and the energy consumption, 5 mA cm^{-2} was suggested as the optimal value for efficient mineralization of DR23 under fixed experimental conditions.

(Figure 7)

4. Conclusion

In summary, the treatment of DR23 was investigated by electrooxidation process in a batch reactor using different electrode configurations in operating conditions of current densities (2.5, 5, 10, and 15 mA cm^{-2}) under values of pH about 3.00, 5.00, 6.00, 7.00, 9.00, and 11.00, and 25 mM NaCl or 12.5 mM Na_2SO_4 as the supporting electrolyte, at 20 °C. The effectiveness of different electrode combinations was compared during the degradation and mineralization of DR23 solution. The results demonstrate that using BDD, Ti_4O_7, or DSA

anodes coupled with CG or SS cathode is found to be helpful for a good discoloration in NaCl medium. In addition, the discoloration rate increases by increasing the electrolysis time, current density, concentration of supporting electrolyte, and decreases by increasing the pH and the concentration of the dye. The best mineralization efficiency obtained for DR23 solutions was achieved with the BDD/CG, followed by BDD/SS with slight efficiency when using CG cathode in both saline solutions. The mineralization of 60 mg L^{-1} of DR23 with BDD/CG system reaches about 86% of TOC removal in either chloride or sulfate solution, using 5 mA cm^{-2} at 6 h of electrolysis time. From MCE% and the energy consumption, 5 mA cm^{-2} was suggested as an optimal value for efficient mineralization of DR23 under fixed experimental conditions using BDD/CG system. The energy consumption and MCE% were 2.05 kWh g^{-1} TOC and 2.5%, and 2.6 kWh g^{-1} TOC and 2.6%, using NaCl and Na_2SO_4, respectively, after 6h of treatment.

The future trend and perspective of this study should focus on the identification of aliphatic intermediates and inorganic ions to propose a mineralization pathway of DR23 and investigate the ecotoxicity assessment of the final effluent to verify that toxicity has been efficiently removed. Likewise, electrochemical behavior of the studied anodes and formed active species in chloride and sulfate salts seem to be of importance. In addition, a comparison between electrooxidation and other processes such as electro-Fenton process will be performed to enhance the efficiency and reduce the treatment time.

Acknowledgements

The authors would like to thank the University of Ibn Zohr Agadir for making all the necessary resources available for this work. F.E. Titchou thanks CNRST for providing the fellowship. This work is done in the framework of the European ERANET MED Water-13_043 project SETPROpER: (Sustainable treatment processes of effluents for reuse of water

563 in agriculture) with the financial support of MOROCCAN MESRSFC. The authors also thank
564 Saint Gobain CREE Company for supplying the Ti_4O_7 anodes.

565

566 **Conflict of interest**

567 On behalf of all authors, the corresponding author states that there is no conflict of interest.

568 **References**

569 [1] M. Panizza, A. Barbucci, R. Ricotti, G. Cerisola, Electrochemical degradation of
570 methylene blue, Sep. Purif. Technol. 54 (2007) 382–387.
571 https://doi.org/10.1016/j.seppur.2006.10.010.
572 [2] E. do Vale-Júnior, S. Dosta, I.G. Cano, J.M. Guilemany, S. Garcia-Segura, C.A.
573 Martínez-Huitle, Acid blue 29 decolorization and mineralization by anodic oxidation
574 with a cold gas spray synthesized Sn–Cu–Sb alloy anode, Chemosphere. 148 (2016) 47–
575 54. https://doi.org/10.1016/j.chemosphere.2016.01.015.
576 [3] Z. Yousefi, A. Zafarzadeh, R.A. Mohammadpour, E. Zarei, N. Mengelizadeh, A.
577 Ghezel, Electrochemical removal of acid red 18 dye from synthetic wastewater using a
578 three-dimensional electrochemical reactor, Desalination Water Treat. 165 (2019) 352–
579 361. https://doi.org/10.5004/dwt.2019.24502.
580 [4] S. Chatterjee, N. Guha, S. Krishnan, A.K. Singh, P. Mathur, D.K. Rai, Selective and
581 Recyclable Congo Red Dye Adsorption by Spherical Fe3O4 Nanoparticles
582 Functionalized with 1,2,4,5-Benzenetetracarboxylic Acid, Sci. Rep. 10 (2020) 111.
583 https://doi.org/10.1038/s41598-019-57017-2.
584 [5] F.E. Titchou, R. Ait Akbour, A. Assabbane, M. Hamdani, Removal of cationic dye from
585 aqueous solution using Moroccan pozzolana as adsorbent: Isotherms, kinetic studies, and

application on real textile wastewater treatment, Groundw. Sustain. Dev. 11 (2020) 100405. https://doi.org/10.1016/j.gsd.2020.100405.

[6] R. Ait Akbour, J.E. Gaayda, F.E. Titchou, A. Khenifi, H. Afanga, A. Farahi, P.-S. Yap, M.B.S. Forte, M. Hamdani, Adsorption of anionic dyes from aqueous solution using polyelectrolyte PDAD-MAC- modified-montmorillonite clay, Desalination Water Treat. 208 (2020) 407–422. https://doi.org/doi: 10.5004/dwt.2020.26446.

[7] J. El Gaayda, R. Ait Akbour, F.E. Titchou, H. Afanga, H. Zazou, C. Swanson, M. Hamdani, Uptake of an anionic dye from aqueous solution by aluminum oxide particles: Equilibrium, kinetic, and thermodynamic studies, Groundw. Sustain. Dev. 12 (2020) 100540. https://doi.org/10.1016/j.gsd.2020.100540.

[8] F.E. Titchou, H. Afanga, H. Zazou, R. Ait Akbour, M. Hamdani, Batch elimination of cationic dye from aqueous solution by electrocoagulation process, Mediterr. J. Chem. 10 (2020) 1–12. https://doi.org/10.13171/mjc10102001201163mh.

[9] H. Afanga, H. Zazou, F.E. Titchou, Y. Rakhila, R. Ait Akbour, A. Elmchaouri, J. Ghanbaja, M. Hamdani, Integrated electrochemical processes for textile industry wastewater treatment: system performances and sludge settling characteristics, Sustain. Environ. Res. 30 (2020) 2. https://doi.org/10.1186/s42834-019-0043-2.

[10] M.M. Emamjomeh, H.A. Jamali, Z. Naghdali, M. Mousazadeh, Efficiency of Electrocoagulation, Sedimentation and Filtration Hybrid Process in Removing Chemical Oxygen Demand and Turbidity from Carwash Industrial Wastewater: Optimization by Response Surface Methodology, J. Mazandaran Univ. Med. Sci. 29 (2019) 106–120.

[11] M.M. Emamjomeh, H. Jamali, Z. Naghdali, M. Mousazadeh, Carwash wastewater treatment by the application of an environmentally friendly hybrid system: an experimental design approach, 160 (2019) 171–177. https://doi.org/10.5004/DWT.2019.24382.

[12] M. Emamjomeh, S. Kakavand, H. Jamali, S.M. Alizadeh, M. Safdari, S.E.S. Mousavi, K.S. Hashim, M. Mousazadeh, The treatment of printing and packaging wastewater by electrocoagulation– flotation: the simultaneous efficacy of critical parameters and economics, Desalination Water Treat. 205 (2020) 161–174. https://doi.org/10.5004/dwt.2020.26339.

[13] F.E. Titchou, H. Zazou, H. Afanga, J. El Gaayda, R.A. Akbour, M. Hamdani, Removal of Persistent Organic Pollutants (POPs) from Water and Wastewater by Adsorption and Electrocoagulation Process, Groundw. Sustain. Dev. 13 (2021) 100575. https://doi.org/10.1016/j.gsd.2021.100575.

[14] E. Petrucci, L. Di Palma, R. Lavecchia, A. Zuorro, Treatment of diazo dye Reactive Green 19 by anodic oxidation on a boron-doped diamond electrode, J. Ind. Eng. Chem. 26 (2015) 116–121. https://doi.org/10.1016/j.jiec.2014.11.022.

[15] C.A. Martínez-Huitle, S. Ferro, Electrochemical oxidation of organic pollutants for the wastewater treatment: direct and indirect processes, Chem Soc Rev. 35 (2006) 1324–1340. https://doi.org/10.1039/B517632H.

[16] C.A. Martínez-Huitle, M. Panizza, Electrochemical oxidation of organic pollutants for wastewater treatment, Curr. Opin. Electrochem. 11 (2018) 62–71. https://doi.org/10.1016/j.coelec.2018.07.010.

[17] S.O. Ganiyu, C.A. Martínez-Huitle, The use of renewable energies driving electrochemical technologies for environmental applications, Curr. Opin. Electrochem. 22 (2020) 211–220. https://doi.org/10.1016/j.coelec.2020.07.007.

[18] C. Candia-Onfray, S. Rojas, M.V.B. Zanoni, R. Salazar, An updated review of metal–organic framework materials in photo(electro)catalytic applications: From CO2 reduction to wastewater treatments, Curr. Opin. Electrochem. 26 (2021) 100669. https://doi.org/10.1016/j.coelec.2020.100669.

[19] S.O. Ganiyu, C.A. Martínez-Huitle, M.A. Rodrigo, Renewable energies driven electrochemical wastewater/soil decontamination technologies: A critical review of fundamental concepts and applications, Appl. Catal. B Environ. 270 (2020) 118857. https://doi.org/10.1016/j.apcatb.2020.118857.

[20] A. Thiam, I. Sirés, J.A. Garrido, R.M. Rodríguez, E. Brillas, Effect of anions on electrochemical degradation of azo dye Carmoisine (Acid Red 14) using a BDD anode and air-diffusion cathode, Sep. Purif. Technol. 140 (2015) 43–52. https://doi.org/10.1016/j.seppur.2014.11.012.

[21] H. Zazou, N. Oturan, M. Sönmez Çelebi, M. Hamdani, M.A. Oturan, Cold incineration of 1,2-dichlorobenzene in aqueous solution by electrochemical advanced oxidation using DSA/Carbon felt, Pt/Carbon felt and BDD/Carbon felt cells, Sep. Purif. Technol. 208 (2019) 184–193. https://doi.org/10.1016/j.seppur.2018.03.030.

[22] I. Sirés, E. Brillas, Upgrading and expanding the electro-Fenton and related processes, Curr. Opin. Electrochem. 27 (2021) 100686. https://doi.org/10.1016/j.coelec.2020.100686.

[23] H. Afanga, H. Zazou, F.E. Titchou, J.E. Gaayda, F. Sopaj, R.A. Akbour, M. Hamdani, Electrochemical oxidation of Naphthol Blue Black with different supporting electrolytes using a BDD /carbon felt cell, J. Environ. Chem. Eng. 9 (2021) 104498. https://doi.org/10.1016/j.jece.2020.104498.

[24] F.E. Titchou, H. Zazou, H. Afanga, J.E. Gaayda, R. Ait Akbour, P.V. Nidheesh, M. Hamdani, An overview on the elimination of organic contaminants from aqueous systems using electrochemical advanced oxidation processes, J. Water Process Eng. 41 (2021) 102040. https://doi.org/10.1016/j.jwpe.2021.102040.

[25] M.A. Oturan, Outstanding performances of the BDD film anode in electro-Fenton process: Applications and comparative performance, Curr. Opin. Solid State Mater. Sci. 25 (2021) 100925. https://doi.org/10.1016/j.cossms.2021.100925.

[26] P.V. Nidheesh, M. Zhou, M.A. Oturan, An overview on the removal of synthetic dyes from water by electrochemical advanced oxidation processes, Chemosphere. 197 (2018) 210–227. https://doi.org/10.1016/j.chemosphere.2017.12.195.

[27] C.A. Martínez-Huitle, M.A. Rodrigo, I. Sirés, O. Scialdone, Single and coupled electrochemical processes and reactors for the abatement of organic water pollutants: A critical review, Chem. Rev. 115 (2015) 13362–13407. https://doi.org/10.1021/acs.chemrev.5b00361.

[28] Y. Yavuz, A. Savaş Koparal, Ü.B. Öğütveren, Electrochemical oxidation of Basic Blue 3 dye using a diamond anode: evaluation of colour, COD and toxicity removal, J. Chem. Technol. Biotechnol. 86 (2011) 261–265. https://doi.org/10.1002/jctb.2512.

[29] J.L. Nava, F. Núñez, I. González, Electrochemical incineration of p-cresol and o-cresol in the filter-press-type FM01-LC electrochemical cell using BDD electrodes in sulfate media at pH 0, Electrochimica Acta. 52 (2007) 3229–3235. https://doi.org/10.1016/j.electacta.2006.09.072.

[30] M. Villanueva-Rodríguez, A. Hernández-Ramírez, J.M. Peralta-Hernández, E.R. Bandala, M.A. Quiroz-Alfaro, Enhancing the electrochemical oxidation of acid-yellow 36 azo dye using boron-doped diamond electrodes by addition of ferrous ion, J. Hazard. Mater. 167 (2009) 1226–1230. https://doi.org/10.1016/j.jhazmat.2008.12.137.

[31] A.M.S. Solano, S. Garcia-Segura, C.A. Martínez-Huitle, E. Brillas, Degradation of acidic aqueous solutions of the diazo dye Congo Red by photo-assisted electrochemical processes based on Fenton's reaction chemistry, Appl. Catal. B Environ. 168–169 (2015) 559–571. https://doi.org/10.1016/j.apcatb.2015.01.019.

[32] S. Trasatti, Electrocatalysis: understanding the success of DSA®, Electrochimica Acta. 45 (2000) 2377–2385. https://doi.org/10.1016/S0013-4686(00)00338-8.

[33] R. Salazar, M.S. Ureta-Zañartu, C. González-Vargas, C. do N. Brito, C.A. Martinez-Huitle, Electrochemical degradation of industrial textile dye disperse yellow 3: Role of electrocatalytic material and experimental conditions on the catalytic production of oxidants and oxidation pathway, Chemosphere. 198 (2018) 21–29. https://doi.org/10.1016/j.chemosphere.2017.12.092.

[34] S.O. Ganiyu, N. Oturan, S. Raffy, M. Cretin, C. Causserand, M.A. Oturan, Efficiency of plasma elaborated sub-stoichiometric titanium oxide (Ti4O7) ceramic electrode for advanced electrochemical degradation of paracetamol in different electrolyte media, Sep. Purif. Technol. 208 (2019) 142–152. https://doi.org/10.1016/j.seppur.2018.03.076.

[35] S.O. Ganiyu, N. Oturan, S. Raffy, G. Esposito, E.D. van Hullebusch, M. Cretin, M.A. Oturan, Use of Sub-stoichiometric Titanium Oxide as a Ceramic Electrode in Anodic Oxidation and Electro-Fenton Degradation of the Beta-blocker Propranolol: Degradation Kinetics and Mineralization Pathway, Electrochimica Acta. 242 (2017) 344–354. https://doi.org/10.1016/j.electacta.2017.05.047.

[36] A. El-Ghenymy, F. Centellas, J.A. Garrido, R.M. Rodríguez, I. Sirés, P.L. Cabot, E. Brillas, Decolorization and mineralization of Orange G azo dye solutions by anodic oxidation with a boron-doped diamond anode in divided and undivided tank reactors, Electrochimica Acta. 130 (2014) 568–576. https://doi.org/10.1016/j.electacta.2014.03.066.

[37] S. Ammar, R. Abdelhedi, C. Flox, C. Arias, E. Brillas, Electrochemical degradation of the dye indigo carmine at boron-doped diamond anode for wastewaters remediation, Environ. Chem. Lett. 4 (2006) 229–233. https://doi.org/10.1007/s10311-006-0053-2.

[38] M. Hamza, R. Abdelhedi, E. Brillas, I. Sirés, Comparative electrochemical degradation of the triphenylmethane dye Methyl Violet with boron-doped diamond and Pt anodes, J. Electroanal. Chem. 627 (2009) 41–50. https://doi.org/10.1016/j.jelechem.2008.12.017.

[39] D. Jager, D. Kupka, M. Vaclavikova, L. Ivanicova, G. Gallios, Degradation of Reactive Black 5 by electrochemical oxidation, Chemosphere. 190 (2018) 405–416. https://doi.org/10.1016/j.chemosphere.2017.09.126.

[40] G. Wang, Y. Liu, J. Ye, Z. Lin, X. Yang, Electrochemical oxidation of methyl orange by a Magnéli phase Ti4O7 anode, Chemosphere. 241 (2020) 125084. https://doi.org/10.1016/j.chemosphere.2019.125084.

[41] S. Song, L. Xu, Z. He, H. Ying, J. Chen, X. Xiao, B. Yan, Photocatalytic degradation of C.I. Direct Red 23 in aqueous solutions under UV irradiation using SrTiO3/CeO2 composite as the catalyst, J. Hazard. Mater. 152 (2008) 1301–1308. https://doi.org/10.1016/j.jhazmat.2007.08.004.

[42] R. Byberg, J. Cobb, L.D. Martin, R.W. Thompson, T.A. Camesano, O. Zahraa, M.N. Pons, Comparison of photocatalytic degradation of dyes in relation to their structure, Environ. Sci. Pollut. Res. 20 (2013) 3570–3581. https://doi.org/10.1007/s11356-013-1551-y.

[43] D.N. Clausen, I.S. Scarmínio, K. Takashima, Optimization and effects of some electron acceptors on the photocatalytic degradation of direct red 23 azo dye, J. Chil. Chem. Soc. 54 (2009) 289-294. https://doi.org/10.4067/S0717-97072009000300018.

[44] L. Ghalamchi, M.H. Rasoulifard, Immobilization of Fe3O4/TiO2 nanocomposite thin layer on the glass tubes in a component parabolic collector for the treatment of DR23, Int. J. Environ. Sci. Technol. 16 (2019) 7509–7522. https://doi.org/10.1007/s13762-018-2169-x.

[45] N. Sobana, K. Selvam, M. Swaminathan, Optimization of photocatalytic degradation conditions of Direct Red 23 using nano-Ag doped TiO2, Sep. Purif. Technol. 62 (2008) 648–653. https://doi.org/10.1016/j.seppur.2008.03.002.

[46] I. Grčić, S. Papić, D. Mesec, N. Koprivanac, D. Vujević, The kinetics and efficiency of UV assisted advanced oxidation of various types of commercial organic dyes in water, J. Photochem. Photobiol. Chem. 273 (2014) 49–58. https://doi.org/10.1016/j.jphotochem.2013.09.009.

[47] N. Liu, L. Zhang, Y. Xue, J. Lv, Q. Yu, X. Yuan, Nitrogen-doped carbon material as a catalyst for the degradation of direct red23 based on persulfate oxidation, Sep. Purif. Technol. 184 (2017) 213–219. https://doi.org/10.1016/j.seppur.2017.04.045.

[48] M. Torkaman, R. Moradi, B. Keyvani, Photocatalytic degradation azo dye direct red 23 using carbon nanotubes particles by uv/h2o2 process in batch photoreactor, Rev. Roum. Chim. 61 (2016) 763-772.

[49] N.M. Mahmoodi, Photocatalytic Degradation of Dyes Using Carbon Nanotube and Titania Nanoparticle, Water. Air. Soil Pollut. 224 (2013) 1612. https://doi.org/10.1007/s11270-013-1612-3.

[50] B. Hayati, N.M. Mahmoodi, M. Arami, F. Mazaheri, Dye Removal from Colored Textile Wastewater by Poly(propylene imine) Dendrimer: Operational Parameters and Isotherm Studies: Dye Removal from Colored Textile Wastewater, CLEAN - Soil Air Water. 39 (2011) 673–679. https://doi.org/10.1002/clen.201000182.

[51] N. Khan, Q. Husain, Continuous degradation of Direct Red 23 by calcium pectate–bound Ziziphus mauritiana peroxidase: identification of metabolites and degradation routes, Environ. Sci. Pollut. Res. 26 (2019) 3517–3529. https://doi.org/10.1007/s11356-018-3847-4.

[52] A.R. Khataee, B. Vahid, B. Behjati, M. Safarpour, Treatment of a dye solution using photoelectro-fenton process on the cathode containing carbon nanotubes under recirculation mode: Investigation of operational parameters and artificial neural network modeling, Environ. Prog. Sustain. Energy. 32 (2013) 557–563. https://doi.org/10.1002/ep.11657.

[53] Reza Moradi, Amin Ganjali, Synthesis of Fe3O4 Nanoparticles and Their Application in Photo-Fenton Degradation of Direct Red 23 Dye in Aqueous Solutions, Russ. J. Phys. Chem. A. 93 (2019) 2789–2797. https://doi.org/10.1134/S0036024419130211.

[54] F.E. Titchou, H. Zazou, H. Afanga, J.E. Gaayda, R. Ait Akbour, M. Hamdani, M.A. Oturan, Electro-Fenton process for the removal of Direct Red 23 using BDD anode in chloride and sulfate media, J. Electroanal. Chem. (2021) 115560. https://doi.org/10.1016/j.jelechem.2021.115560.

[55] M. Mohajerani, M. Mehrvar, F. Ein-Mozaffari, Correlation and prediction of azo dye degradation by nonlinear least-square regression in combined ozonation and ultrasonolysis processes, Water Qual. Res. J. 46 (2011) 250–258. https://doi.org/10.2166/wqrjc.2011.128.

[56] H. Jalife-Jacobo, R. Feria-Reyes, O. Serrano-Torres, S. Gutiérrez-Granados, J.M. Peralta-Hernández, Diazo dye Congo Red degradation using a Boron-doped diamond anode: An experimental study on the effect of supporting electrolytes, J. Hazard. Mater. 319 (2016) 78–83. https://doi.org/10.1016/j.jhazmat.2016.02.056.

[57] S. Liu, H. Song, S. Wei, Q. Liu, X. Li, X. Qian, Effect of direct electrical stimulation on decolorization and degradation of azo dye reactive brilliant red X-3B in biofilm-electrode reactors, Biochem. Eng. J. 93 (2015) 294–302. https://doi.org/10.1016/j.bej.2014.11.002.

780 [58] Z. Hu, J. Cai, G. Song, Y. Tian, M. Zhou, Anodic oxidation of organic pollutants: Anode
781 fabrication, process hybrid and environmental applications, Curr. Opin. Electrochem. 26
782 (2021) 100659. https://doi.org/10.1016/j.coelec.2020.100659.
783 [59] I. Bisschops, H. Spanjers, Literature review on textile wastewater characterisation,
784 Environ. Technol. 24 (2003) 1399–1411. https://doi.org/10.1080/09593330309385684.
785 [60] D.A. Yaseen, M. Scholz, Textile dye wastewater characteristics and constituents of
786 synthetic effluents: a critical review, Int. J. Environ. Sci. Technol. 16 (2019) 1193–1226.
787 https://doi.org/10.1007/s13762-018-2130-z.
788 [61] H. Zazou, N. Oturan, M. Sönmez Çelebi, M. Hamdani, M.A. Oturan, Cold incineration
789 of 1,2-dichlorobenzene in aqueous solution by electrochemical advanced oxidation using
790 DSA/Carbon felt, Pt/Carbon felt and BDD/Carbon felt cells, Sep. Purif. Technol. 208
791 (2019) 184–193. https://doi.org/10.1016/j.seppur.2018.03.030.
792 [62] N. Yu, X. Lu, F. Song, Y. Yao, E. Han, Electrocatalytic degradation of sulfamethazine
793 on IrO2-RuO2 composite electrodes: influencing factors, kinetics and modeling, J.
794 Environ. Chem. Eng. 9 (2021) 105301. https://doi.org/10.1016/j.jece.2021.105301.
795 [63] M. Fryda, Th. Matthee, S. Mulachy, M. Hofer, L. Schafer, I. Troster, Applications of
796 DIACHEM ® Electrodes in Electrolytic Water Treatment, Electrochem. Soc. Interface.
797 12 (2003) 40–44. https://doi.org/10.1149/2.F10031IF.
798 [64] C. Liu, Z. Chen, H. Chen, Z. Miao, M. Fu, Preparation of expanded graphite-based
799 composites by one step impregnation, J. Wuhan Univ. Technol.-Mater Sci Ed. 26 (2011)
800 253–256. https://doi.org/10.1007/s11595-011-0208-2.
801 [65] S.O. Ganiyu, N. Oturan, S. Raffy, M. Cretin, R. Esmilaire, E. van Hullebusch, G.
802 Esposito, M.A. Oturan, Sub-stoichiometric titanium oxide (Ti4O7) as a suitable ceramic
803 anode for electrooxidation of organic pollutants: A case study of kinetics, mineralization

and toxicity assessment of amoxicillin, Water Res. 106 (2016) 171–182. https://doi.org/10.1016/j.watres.2016.09.056.

[66] Y. Ouarda, C. Trellu, G. Lesage, M. Rivallin, P. Drogui, M. Cretin, Electro-oxidation of secondary effluents from various wastewater plants for the removal of acetaminophen and dissolved organic matter, Sci. Total Environ. 738 (2020) 140352. https://doi.org/10.1016/j.scitotenv.2020.140352.

[67] E. Brillas, C.A. Martínez-Huitle, Decontamination of wastewaters containing synthetic organic dyes by electrochemical methods. An updated review, Appl. Catal. B Environ. 166–167 (2015) 603–643. https://doi.org/10.1016/j.apcatb.2014.11.016.

[68] P. Saxena, J. Ruparelia, Influence of supporting electrolytes on electrochemical treatability of reactive black 5 using dimensionally stable anode, J. Inst. Eng. India Ser. A. 100 (2019) 299–310. https://doi.org/10.1007/s40030-019-00360-4.

[69] D. Li, J. Tang, X. Zhou, J. Li, X. Sun, J. Shen, L. Wang, W. Han, Electrochemical degradation of pyridine by Ti/SnO2–Sb tubular porous electrode, Chemosphere. 149 (2016) 49–56. https://doi.org/10.1016/j.chemosphere.2016.01.078.

[70] A.S. Abdalrhman, Electro-oxidation by graphite anode for naphthenic acids degradation, biodegradability enhancement and toxicity reduction, Sci. Total Environ. 671 (2019) 270-279. https://doi.org/10.1016/j.scitotenv.2019.03.262

[71] M. Rueffer, D. Bejan, N.J. Bunce, Graphite: An active or an inactive anode?, Electrochimica Acta. 56 (2011) 2246–2253. https://doi.org/10.1016/j.electacta.2010.11.071.

[72] G. Divyapriya, P.V. Nidheesh, Electrochemically generated sulfate radicals by boron doped diamond and its environmental applications, Curr. Opin. Solid State Mater. Sci. 25 (2021) 100921. https://doi.org/10.1016/j.cossms.2021.100921.

[73] S.O. Ganiyu, C.A. Martínez-Huitle, M.A. Oturan, Electrochemical advanced oxidation processes for wastewater treatment: Advances in formation and detection of reactive species and mechanisms, Curr. Opin. Electrochem. 27 (2021) 100678. https://doi.org/10.1016/j.coelec.2020.100678.

[74] K.C. de Freitas Araújo, D.R. da Silva, E.V. dos Santos, H. Varela, C.A. Martínez-Huitle, Investigation of persulfate production on BDD anode by understanding the impact of water concentration, J. Electroanal. Chem. 860 (2020) 113927. https://doi.org/10.1016/j.jelechem.2020.113927.

[75] D. Zhi, Y. Lin, L. Jiang, Y. Zhou, A. Huang, J. Yang, L. Luo, Remediation of persistent organic pollutants in aqueous systems by electrochemical activation of persulfates: A review, J. Environ. Manage. 260 (2020) 110125. https://doi.org/10.1016/j.jenvman.2020.110125.

[76] J. Cai, T. Niu, P. Shi, G. Zhao, Boron-Doped Diamond for Hydroxyl Radical and Sulfate Radical Anion Electrogeneration, Transformation, and Voltage-Free Sustainable Oxidation, Small. 15 (2019) 1900153. https://doi.org/10.1002/smll.201900153.

[77] S. Wacławek, H.V. Lutze, K. Grübel, V.V.T. Padil, M. Černík, Dionysios.D. Dionysiou, Chemistry of persulfates in water and wastewater treatment: A review, Chem. Eng. J. 330 (2017) 44–62. https://doi.org/10.1016/j.cej.2017.07.132.

[78] J. Lee, U. von Gunten, J.-H. Kim, Persulfate-Based Advanced Oxidation: Critical Assessment of Opportunities and Roadblocks, Environ. Sci. Technol. 54 (2020) 3064–3081. https://doi.org/10.1021/acs.est.9b07082.

[79] G. Farshid, M. Mahsa, Application of peroxymonosulfate and its activation methods for degradation of environmental organic pollutants: review, Chem Eng J. 310 (2017) 41–62. https://doi.org/10.1016/j.cej.2016.10.064.

[80] K. Groenen Serrano, A critical review on the electrochemical production and use of peroxo-compounds, Curr. Opin. Electrochem. 27 (2021) 100679. https://doi.org/10.1016/j.coelec.2020.100679.

[81] S. Giannakis, K.-Y.A. Lin, F. Ghanbari, A review of the recent advances on the treatment of industrial wastewaters by Sulfate Radical-based Advanced Oxidation Processes (SR-AOPs), Chem. Eng. J. 406 (2021) 127083. https://doi.org/10.1016/j.cej.2020.127083.

[82] C. Zhu, C. Jiang, S. Chen, R. Mei, X. Wang, J. Cao, L. Ma, B. Zhou, Q. Wei, G. Ouyang, Z. Yu, K. Zhou, Ultrasound enhanced electrochemical oxidation of alizarin red S on boron doped diamond (BDD) anode: Effect of degradation process parameters, Chemosphere. 209 (2018) 685–695. https://doi.org/10.1016/j.chemosphere.2018.06.137.

[83] A.H. Degaki, G.F. Pereira, R.C. Rocha-Filho, N. Bocchi, S.R. Biaggio, Effect of Specific Active Chlorine Species and Temperature on the Electrochemical Degradation of the Reactive Blue 19 Dye Using a Boron-Doped Diamond or DSA Anode in a Flow Reactor, Electrocatalysis. 5 (2014) 8–15. https://doi.org/10.1007/s12678-013-0156-z.

[84] C.Y. Cheng, G.H. Kelsall, Models of hypochlorite production in electrochemical reactors with plate and porous anodes, J. Appl. Electrochem. 37 (2007) 1203–1217. https://doi.org/10.1007/s10800-007-9364-7.

[85] C.M. Dominguez, N. Oturan, A. Romero, A. Santos, M.A. Oturan, Lindane degradation by electrooxidation process: Effect of electrode materials on oxidation and mineralization kinetics, Water Res. 135 (2018) 220–230. https://doi.org/10.1016/j.watres.2018.02.037.

[86] L. Wang, J. Lu, L. Li, Y. Wang, Q. Huang, Effects of chloride on electrochemical degradation of perfluorooctanesulfonate by Magnéli phase Ti4O7 and boron doped

876 diamond anodes, Water Res. 170 (2020) 115254.
877 https://doi.org/10.1016/j.watres.2019.115254.
878 [87] L. Wang, M. Nickelsen, S.-Y. (Dora) Chiang, S. Woodard, Y. Wang, S. Liang, R. Mora,
879 R. Fontanez, H. Anderson, Q. Huang, Treatment of perfluoroalkyl acids in concentrated
880 wastes from regeneration of spent ion exchange resin by electrochemical oxidation using
881 Magnéli phase Ti4O7 anode, Chem. Eng. J. Adv. 5 (2021) 100078.
882 https://doi.org/10.1016/j.ceja.2020.100078.
883 [88] I. Diouf, O. Dia, M.B. Diedhiou, P. Drogui, A.O. Toure, S.M. Lo, M. Rumeau, C.G.
884 Mar/Diop, Electro-generation of hydrogen peroxide using a graphite cathode from
885 exhausted batteries: study of influential parameters on electro-Fenton process, Environ.
886 Technol. 41 (2020) 1434–1445. https://doi.org/10.1080/09593330.2018.1537309.
887 [89] O. García-Rodríguez, J.A. Bañuelos, A. Rico-Zavala, L.A. Godínez, F.J. Rodríguez-
888 Valadez, Electrocatalytic activity of three carbon materials for the In-situ production of
889 hydrogen peroxide and Its application to the electro-Fenton heterogeneous process, Int.
890 J. Chem. React. Eng. 14 (2016) 843–850. https://doi.org/10.1515/ijcre-2015-0115.
891 [90] W. Yang, M. Zhou, N. Oturan, Y. Li, P. Su, M.A. Oturan, Enhanced activation of
892 hydrogen peroxide using nitrogen doped graphene for effective removal of herbicide
893 2,4-D from water by iron-free electrochemical advanced oxidation, Electrochimica Acta.
894 297 (2019) 582–592. https://doi.org/10.1016/j.electacta.2018.11.196.
895 [91] E. Saputra, S. Muhammad, H. Sun, S. Wang, Activated carbons as green and effective
896 catalysts for generation of reactive radicals in degradation of aqueous phenol, RSC Adv.
897 3 (2013) 21905. https://doi.org/10.1039/c3ra42455c.
898 [92] F. Sopaj, N. Oturan, J. Pinson, F.I. Podvorica, M.A. Oturan, Effect of cathode material
899 on electro-Fenton process efficiency for electrocatalytic mineralization of the antibiotic

900 sulfamethazine, Chem. Eng. J. 384 (2020) 123249.
901 https://doi.org/10.1016/j.cej.2019.123249.
902 [93] W. He, Y. Liu, J. Ye, G. Wang, Electrochemical degradation of azo dye methyl orange
903 by anodic oxidation on Ti4O7 electrodes, J. Mater. Sci. Mater. Electron. 29 (2018)
904 14065–14072. https://doi.org/10.1007/s10854-018-9538-6.
905 [94] A. Kapałka, G. Fóti, C. Comninellis, The importance of electrode material in
906 environmental electrochemistry, Electrochimica Acta. 54 (2009) 2018–2023.
907 https://doi.org/10.1016/j.electacta.2008.06.045.
908 [95] M. Mascia, A. Vacca, S. Palmas, A.M. Polcaro, Kinetics of the electrochemical
909 oxidation of organic compounds at BDD anodes: modelling of surface reactions, J. Appl.
910 Electrochem. 37 (2006) 71–76. https://doi.org/10.1007/s10800-006-9217-9.
911 [96] G.R.P. Malpass, G.R. Salazar-Banda, D.W. Miwa, S.A.S. Machado, A.J. Motheo,
912 Comparing atrazine and cyanuric acid electro-oxidation on mixed oxide and boron-
913 doped diamond electrodes, Environ. Technol. 34 (2013) 1043–1051.
914 https://doi.org/10.1080/09593330.2012.733420.
915 [97] L. Gomes, D.W. Miwa, G.R.P. Malpass, A.J. Motheo, Electrochemical degradation of
916 the dye reactive orange 16 using electrochemical flow-cell, J. Braz. Chem. Soc. 22
917 (2011) 1299–1306. https://doi.org/10.1590/S0103-50532011000700015.
918 [98] D. Rajkumar, B.J. Song, J.G. Kim, Electrochemical degradation of Reactive Blue 19 in
919 chloride medium for the treatment of textile dyeing wastewater with identification of
920 intermediate compounds, Dyes Pigments. 72 (2007) 1–7.
921 https://doi.org/10.1016/j.dyepig.2005.07.015.
922 [99] S. Zeb, S. Hussain, H.A. Khan, Z. Ali, N. Khan, K.I. Khan, F. Ali, S. khan, M. del P.T.
923 Sotomayo, S. Gul, Electrochemical Oxidation of Acid Brown 98 using Ti/Ru0.3Ti0.7O2

924 Composite Anode, Int. J. Electrochem. Sci. 13 (2018) 9428–9440.
925 https://doi.org/10.20964/2018.10.06.
926 [100] D.F. Viana, G.R. Salazar-Banda, M.S. Leite, Electrochemical degradation of Reactive
927 Black 5 with surface response and artificial neural networks optimization models, Sep.
928 Sci. Technol. 53 (2018) 2647–2661. https://doi.org/10.1080/01496395.2018.1463264.
929 [101] C. do N. Brito, D.R. da Silva, S. Garcia-Segura, D.C. de Moura, C.A. Martínez-Huitle,
930 Indirect Electrochemical Oxidation of Reactive Blue 19 Dye as a Model Organic
931 Substrate: Role of Anode Material and Oxidants Electrochemically Generated, J.
932 Electrochem. Soc. 163 (2016) E62–E69. https://doi.org/10.1149/2.0191603jes.
933 [102] M.F. Murrieta, I. Sirés, E. Brillas, J.L. Nava, Mineralization of Acid Red 1 azo dye by
934 solar photoelectro-Fenton-like process using electrogenerated HClO and
935 photoregenerated Fe(II), Chemosphere. 246 (2020) 125697.
936 https://doi.org/10.1016/j.chemosphere.2019.125697.
937 [103] M. Panizza, M.A. Oturan, Degradation of Alizarin Red by electro-Fenton process
938 using a graphite-felt cathode, Electrochimica Acta. 56 (2011) 7084–7087.
939 https://doi.org/10.1016/j.electacta.2011.05.105.
940 [104] J. Wang, D. Zhi, H. Zhou, X. He, D. Zhang, Evaluating tetracycline degradation
941 pathway and intermediate toxicity during the electrochemical oxidation over a Ti/Ti4O7
942 anode, Water Res. 137 (2018) 324–334. https://doi.org/10.1016/j.watres.2018.03.030.
943 [105] J. Cai, M. Zhou, Y. Pan, X. Lu, Degradation of 2,4-dichlorophenoxyacetic acid by
944 anodic oxidation and electro-Fenton using BDD anode: Influencing factors and
945 mechanism, Sep. Purif. Technol. 230 (2020) 115867.
946 https://doi.org/10.1016/j.seppur.2019.115867.

[106] M.H. Abdel-Aziz, M. Bassyouni, M.S. Zoromba, A.A. Alshehri, Removal of dyes from waste solutions by anodic oxidation on an array of horizontal graphite rods anodes, Ind. Eng. Chem. Res. 58 (2019) 1004–1018. https://doi.org/10.1021/acs.iecr.8b05291.

[107] K. Groenen Serrano, Chapter 6 - Indirect Electrochemical Oxidation Using Hydroxyl Radical, Active Chlorine, and Peroxodisulfate, in: C.A. Martínez-Huitle, M.A. Rodrigo, O. Scialdone (Eds.), Electrochem. Water Wastewater Treat., Butterworth-Heinemann, 2018: pp. 133–164. https://doi.org/10.1016/B978-0-12-813160-2.00006-7.

[108] L. Gui, H. Jin, Y. Zheng, R. Peng, Y. Luo, P. Yu, Electrochemical Degradation of Bisphenol A Using Different Modified Anodes Based on Titanium in Aqueous Solution, Int. J. Electrochem. Sci. 13 (2018) 7141–7156. https://doi.org/10.20964/2018.07.76.

[109] G.R. Salazar-Banda, G. de O.S. Santos, I.M. Duarte Gonzaga, A.R. Dória, K.I. Barrios Eguiluz, Developments in electrode materials for wastewater treatment, Curr. Opin. Electrochem. 26 (2021) 100663. https://doi.org/10.1016/j.coelec.2020.100663.

[110] W. Yang, N. Oturan, S. Raffy, M. Zhou, M.A. Oturan, Electrocatalytic generation of homogeneous and heterogeneous hydroxyl radicals for cold mineralization of anti-cancer drug Imatinib, Chem. Eng. J. 383 (2020) 123155. https://doi.org/10.1016/j.cej.2019.123155.

[111] F.C. Moreira, R.A.R. Boaventura, E. Brillas, V.J.P. Vilar, Electrochemical advanced oxidation processes: A review on their application to synthetic and real wastewaters, Appl. Catal. B Environ. 202 (2017) 217–261. https://doi.org/10.1016/j.apcatb.2016.08.037.

970 **Table 1.** Recent studies on decontamination of dye solutions by anodic oxidation method.

Pollutants	**Conditions**	**Maximum degradation**	**References**
Acid red18	-Ti/ Graphite felt/ Granular activated carbon (GAC) in fluidized bed. -Optimal conditions: C_0 =100 mg L^{-1}, 100 mM NaCl, pH = 3, j= 20 mA cm^{-2}, GAC =250 mg L^{-1}	96.5% of color removal and 84.8% of COD removal at 45 min	[3]
Acid blue 29	-Sn-Cu-Sb/SS -Optimal conditions: C_0=60 mg L^{-1}, j=10 mA cm^{-2}, pH= 7, 50 mM Na_2SO_4	100% of COD removal at 600 min	[2]
Orange G	-BDD/SS -Conditions: 100 cm^3 of 0.52-6.34 mM of Orange G azo dye, pH 3, 50 mM Na_2SO_4, and current density between 33.3 and 150 mA cm^{-2}	-100 %TOC removal in less than 330 min operating at j $\geq$ 66.7 mA cm^{-2} -100% Color removal at 396 min-at 150 mA cm^{-2}.	[36]
indigo carmine	-BDD/SS -Conditions: indigo carmine up to 0.9 g L^{-1}, 50 mM Na_2SO_4, pH 3.0-10.0, and 100, 300, and 450 mA at 35◦C.	TOC reduced with current. 100% mineralization drops from 600 min at 100 mA to 300 min at 450 mA.	[37]

Methyl Violet	-BDD or Pt/SS -Conditions: 100 cm^3 of 100 mg L^{-1}, 50 mM Na_2SO_4, pH 3.0-7.4, current density 33.3- 150 mA cm^{-2}	- BDD, >97% TOC decay with 18 Ah dm^{-3} (360 min) at pH 3.0 and 15 Ah dm^{-3} (300 min) at pH 7.4 - Pt TOC decay, close to 22% and 33% at pH 3.0 and 7.4.	[38]
Reactive Black 5	-Ti/RuO_2/IrO_2/TiO_2/SS Optimal conditions: C_0=300 mg L^{-1}, 100 mA cm^{-2}, 8 mM NaCl	-100 % of color removal and 33% of COD decay at 15 min.	[39]
Methyl orange	-Ti_4O_7/ Ti -Conditions: C_0 = 100 mg L^{-1}, 10 mA cm^{-2}, 100 mM NaCl	-Complete color removal and 91.7% COD reached after 5 h electrolysis	[40]

971 **COD:** Chemical Oxygen Demand; **TOC :** Total Organic Carbon; **SS:** stainless steel

972

973

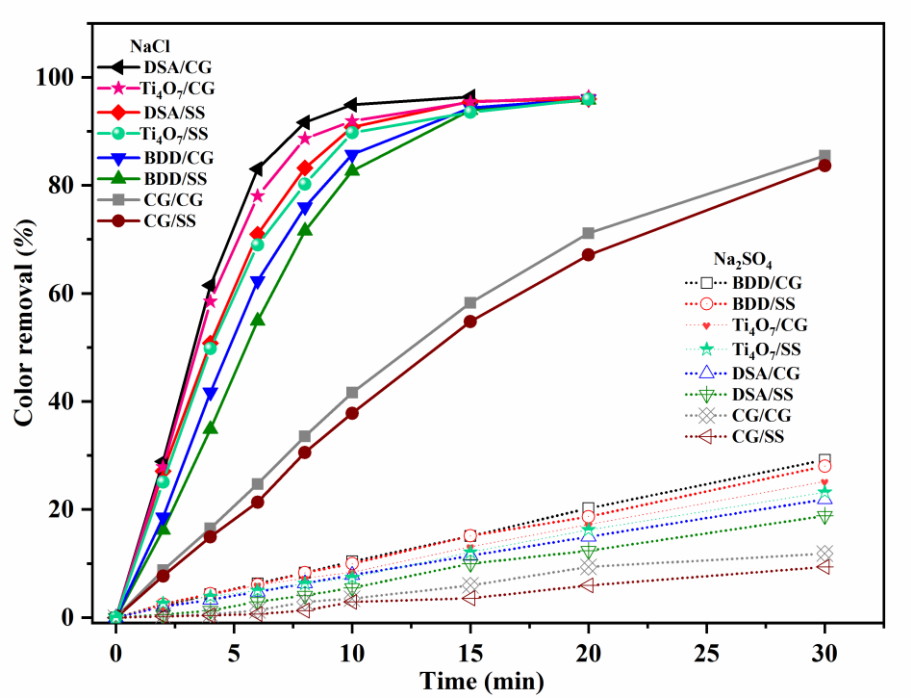

Figure 1: Kinetics of color removal (%) on different electrode materials; 40 mg L^{-1} DR23, 25 mM NaCl or 12.5 mM Na_2SO_4, 8.3 mA cm^{-2}, pH = 6.0.

974

975

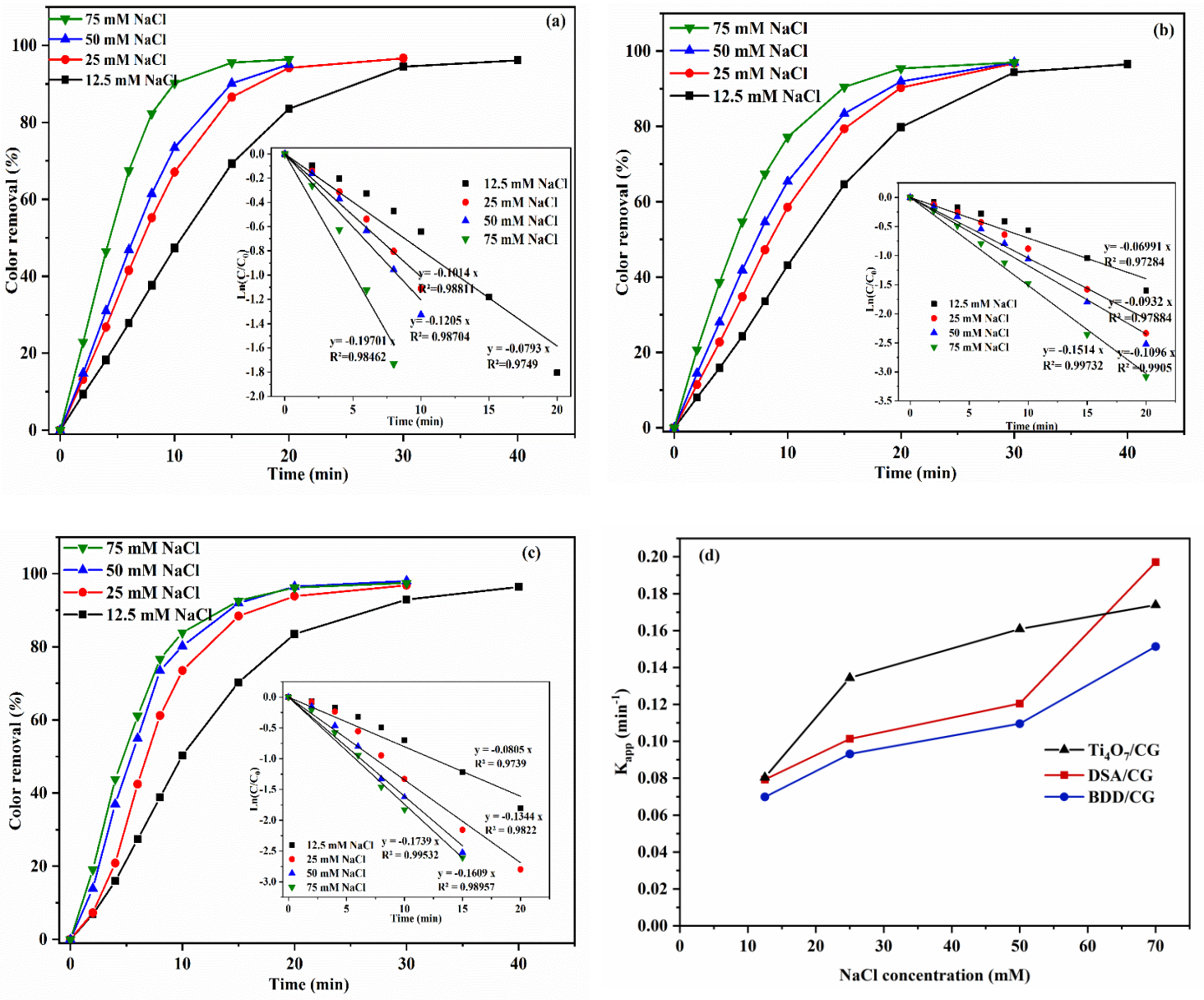

Figure 2: Effect of NaCl concentration, 60 mg L^{-1} DR23, pH = 6.0, 5 mA cm^{-2}, (a) color removal (%), (a): DSA/CG, (b): BDD/CG, (c): Ti_4O_7/CG, and (d): the apparent kinetic rate constants vs. NaCl concentration. The insert panels are the kinetic analysis assuming a pseudo first order reaction.

976

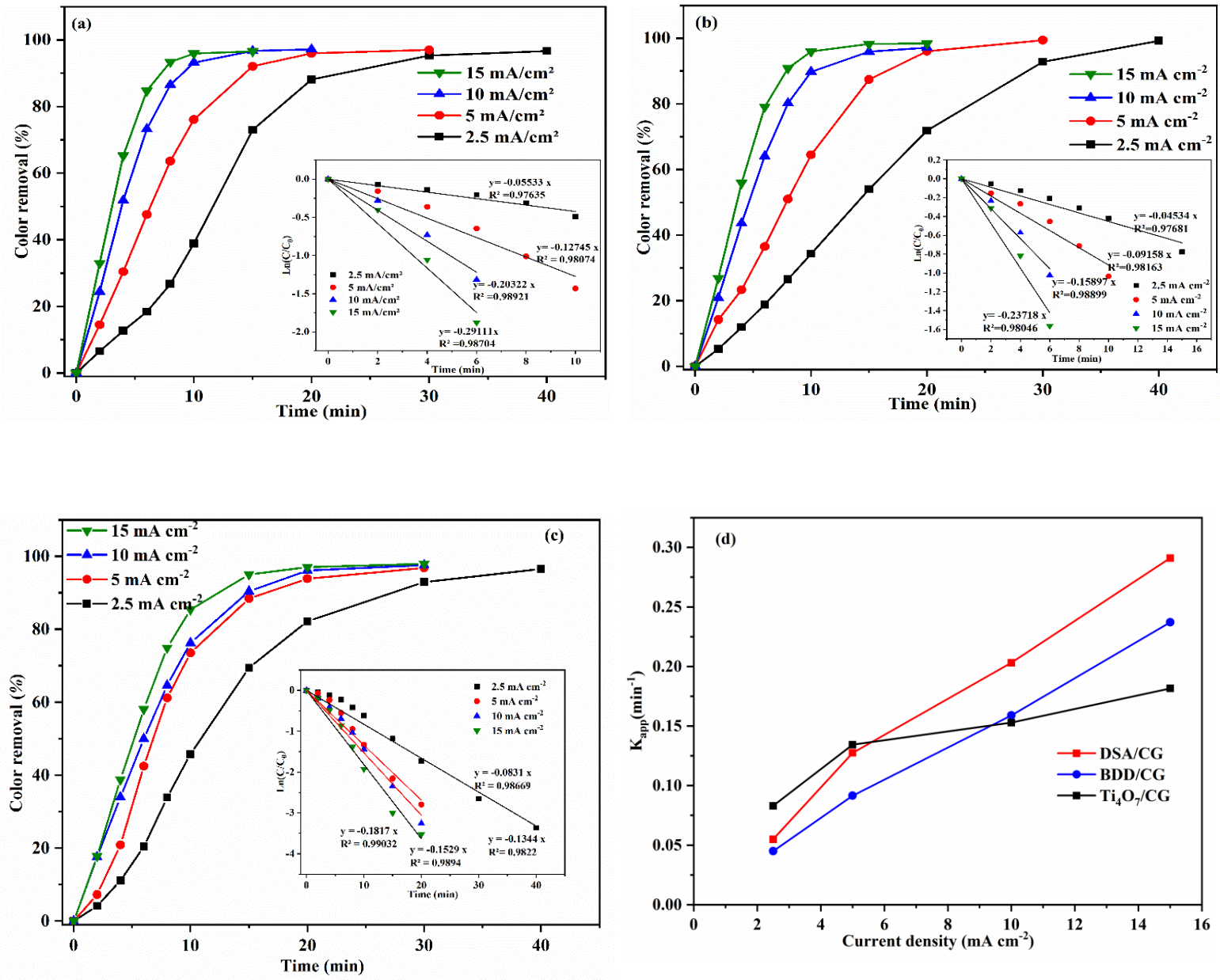

Figure 3: Effect of the current density, 60 mg L^{-1} of DR23, 25 mM NaCl, pH = 5.89, (a): DSA/CG, (b): BDD/CG, (c): Ti_4O_7/CG, and (d): apparent kinetic rate. The insert panels are the kinetic analysis assuming a pseudo first-order reaction.

977

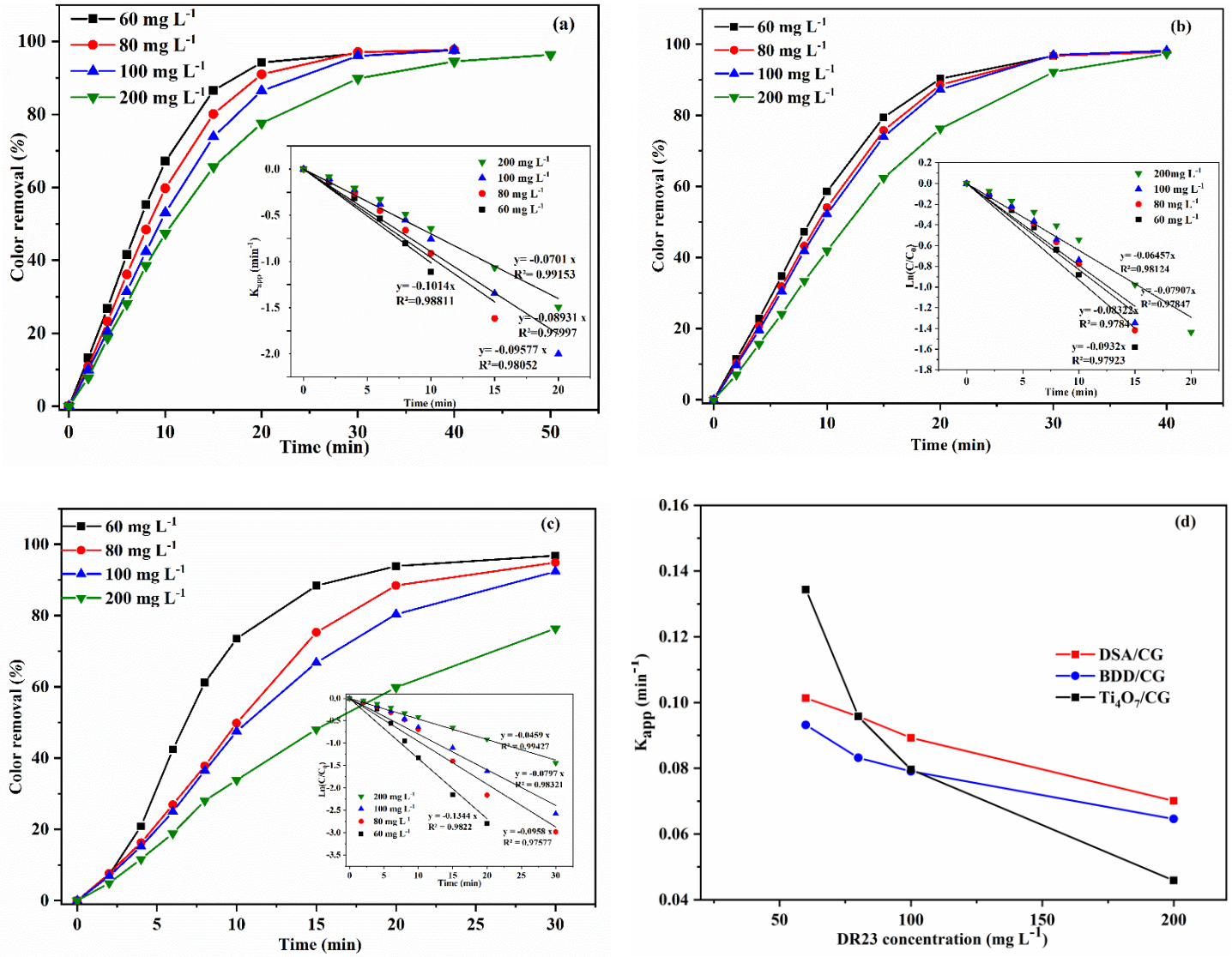

Figure 4: Effect of the initial dye concentration, 25 mM NaCl, pH = 5.89, 5 mA cm^{-2} (a): DSA/CG, (b): BDD/CG, (c): Ti_4O_7/CG, and (d): variation of apparent kinetic rate. The insert panels are the kinetic analysis assuming a pseudo first order reaction.

978

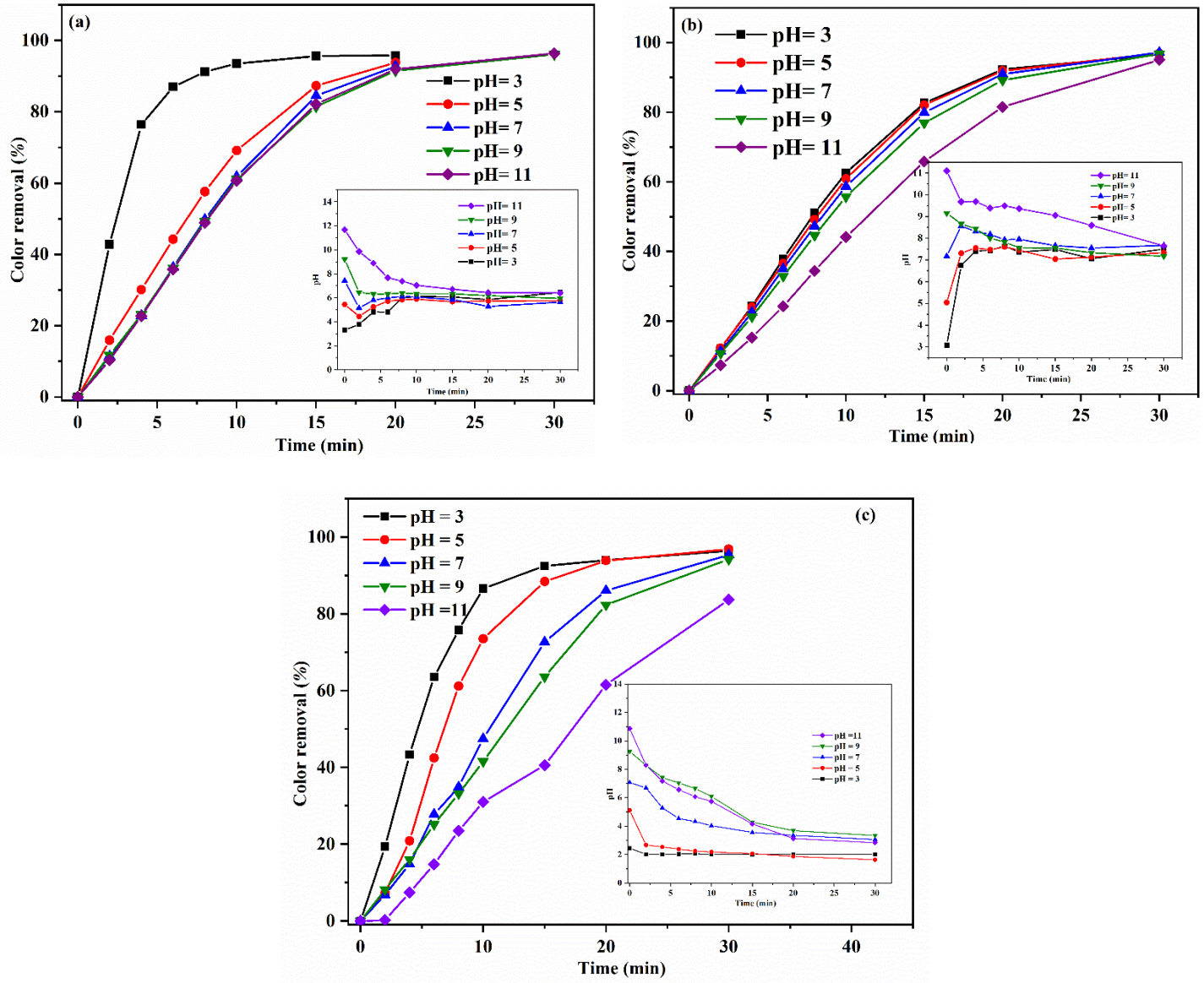

Figure 5: Effect of the initial pH on the color removal, 60 mg L^{-1} of DR23, 25 mM NaCl, 5 mA cm^{-2}. Insert panels: variation of pH vs. time, (a): DSA/CG, (b): BDD/CG, and (c): Ti_4O_7/CG

979

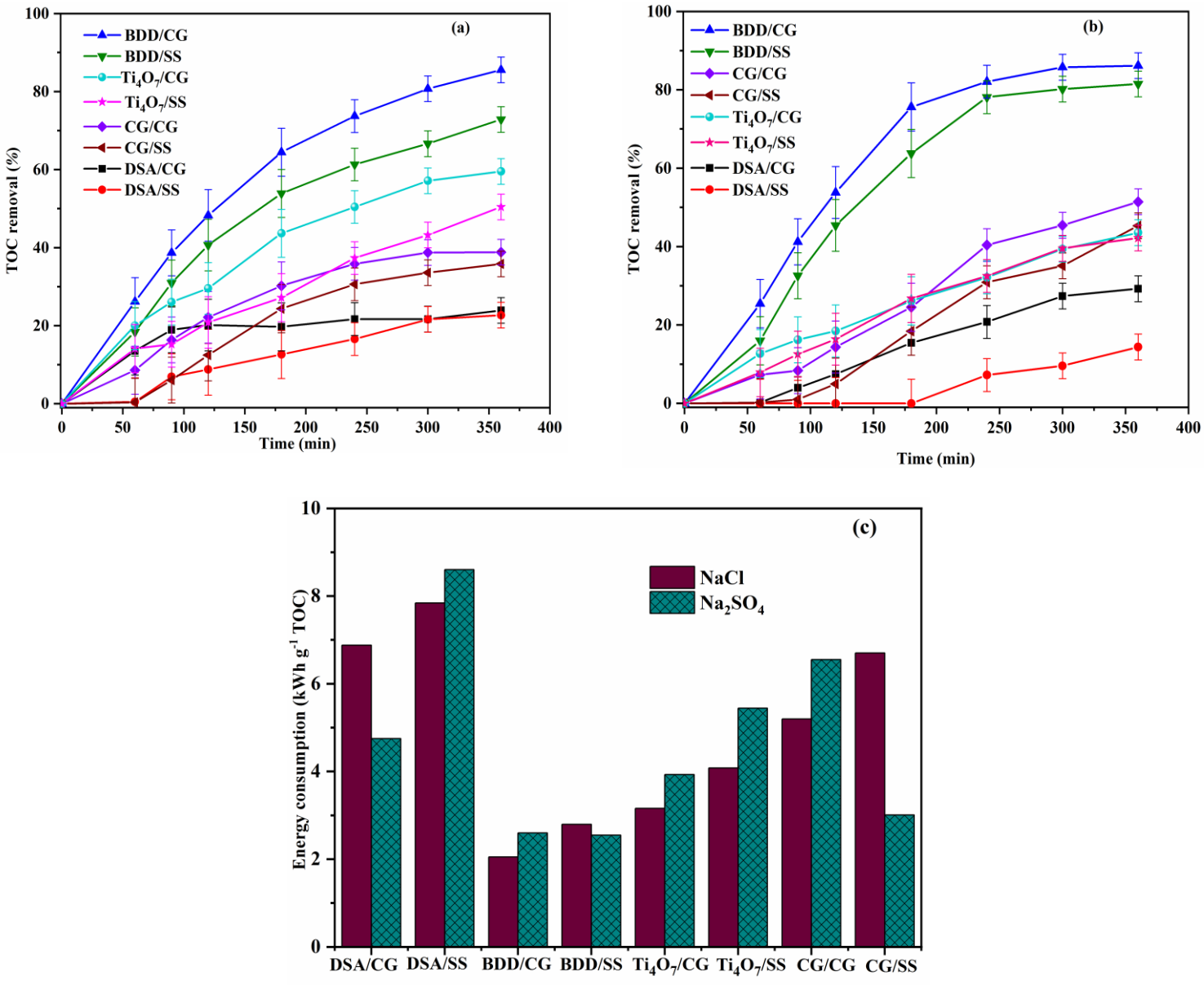

Figure 6: TOC removal vs. electrodes nature, 60 mg L^{-1} of DR23 , pH = 3.00, and 5 mA cm^{-2}, after 6h of electrolysis time, (a): 25 mM NaCl, (b): 12.5 mM Na_2SO_4, (c): Energy consumption for tested systems, kWh g^{-1} TOC

980

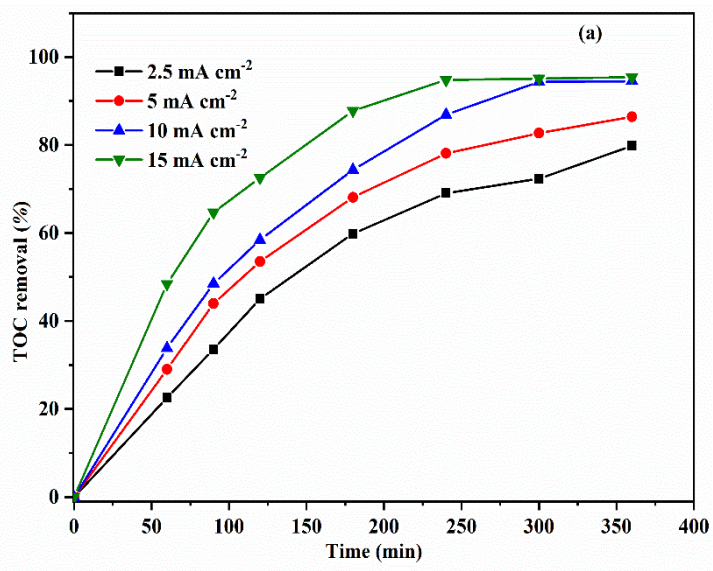
(a)
2.5 mA cm-2
5 mA cm-2
10 mA cm-2
15 mA cm-2
TOC removal (%)
Time (min)

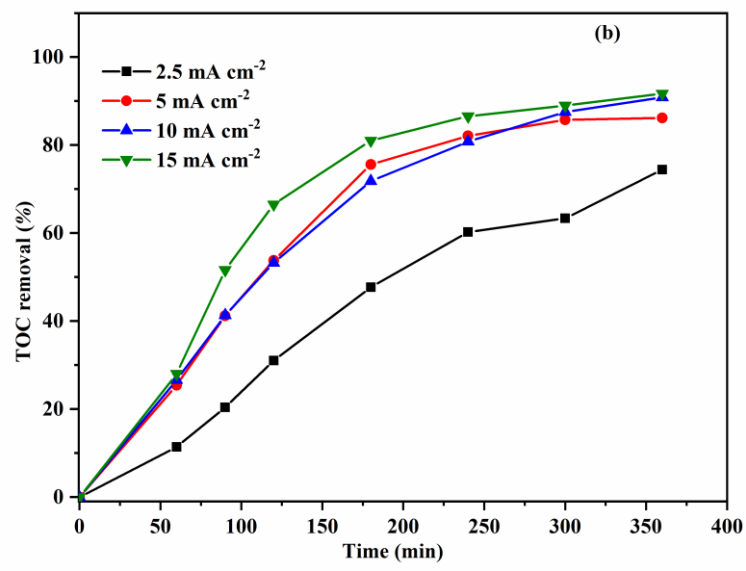
(b)
2.5 mA cm-2
5 mA cm-2
10 mA cm-2
15 mA cm-2
TOC removal (%)
Time (min)

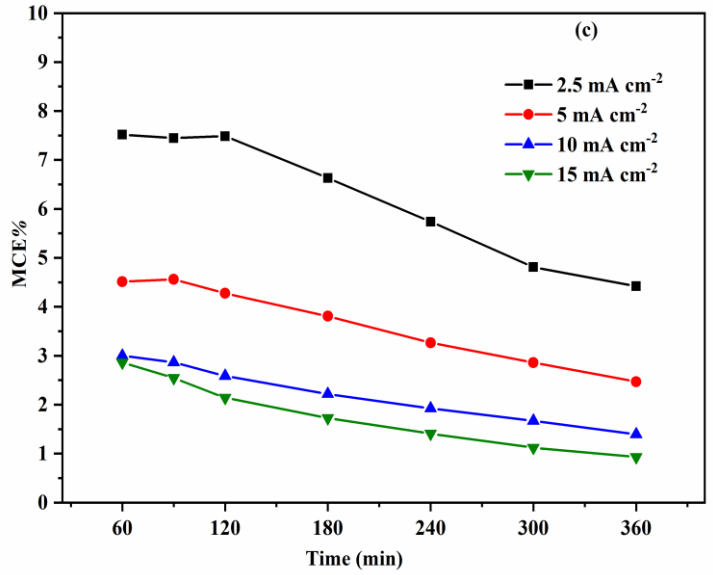
(c)
2.5 mA cm-2
5 mA cm-2
10 mA cm-2
15 mA cm-2
MCE%
Time (min)

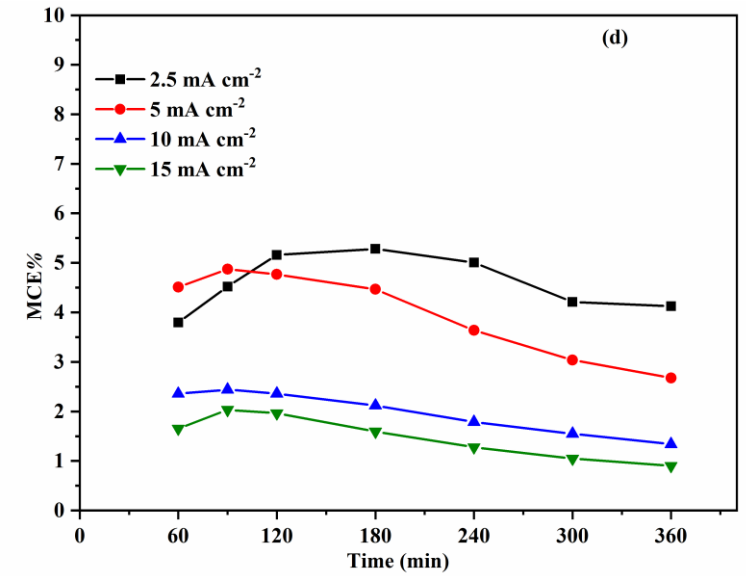
(d)
2.5 mA cm-2
5 mA cm-2
10 mA cm-2
15 mA cm-2
MCE%
Time (min)

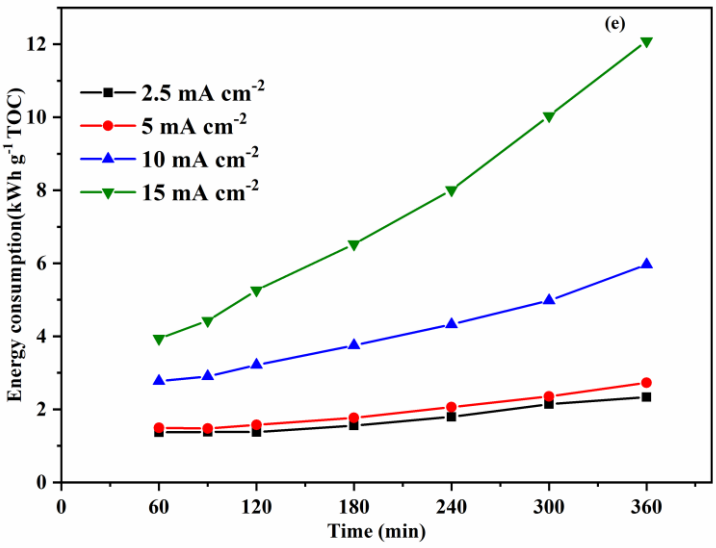
(e)
2.5 mA cm-2
5 mA cm-2
10 mA cm-2
15 mA cm-2
Energy consumption(kWh g-1 TOC)
Time (min)

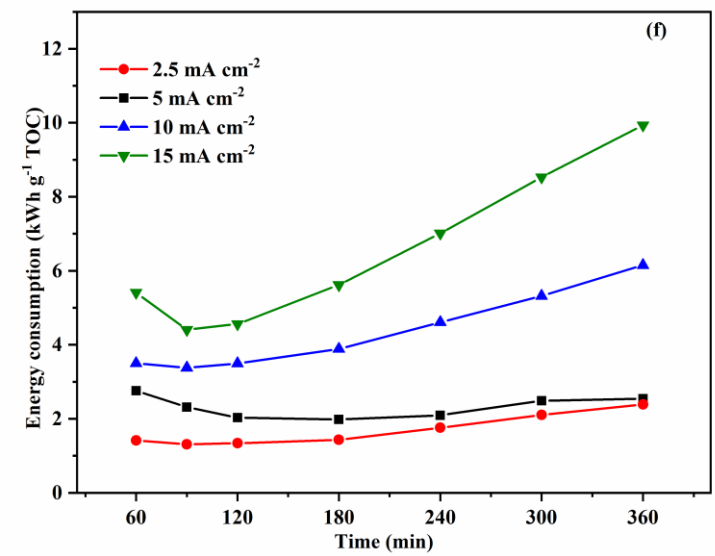
(f)
2.5 mA cm-2
5 mA cm-2
10 mA cm-2
15 mA cm-2
Energy consumption (kWh g-1 TOC)
Time (min)

Figure 7: Effect of current on the mineralization of 60 mg L^{-1} DR23 vs. time, (a, c, e) 25 mM NaCl, (b, d, f) 12.5 mM Na_2SO_4, pH = 3.00, BDD/CG, (a, b) TOC removal, (c, d) mineralization efficiencies (MCE%), (e, f) Energy consumption (kWh g^{-1} TOC)

981